GigaScience

A chromosome-level genome assembly and annotation of the desert horned lizard, Phrynosoma platyrhinos, provides insight into chromosomal rearrangements among reptiles

--Manuscript Draft--

Manuscript Number:	GIGA-D-21-00044R2
Full Title:	A chromosome-level genome assembly and annotation of the desert horned lizard, Phrynosoma platyrhinos, provides insight into chromosomal rearrangements among reptiles
Article Type:	Research
Funding Information:	Miami University — Dr Tereza Jezkova National Science Foundation Graduate Research Fellowship Program (2037786) — Mr Keaka Farleigh
Abstract:	Background . The increasing number of chromosome-level genome assemblies has advanced our knowledge and understanding of macroevolutionary processes. Here, we introduce the genome of the desert horned lizard, Phrynosoma platyrhinos, an iguanid lizard occupying extreme desert conditions of the American southwest. We conduct analysis of the chromosomal structure and composition of this species and compare these features across genomes of 12 other reptiles (5 species of lizards, 3 snakes, 3 turtles, and 1 bird). Findings . The desert horned lizard genome was sequenced using Illumina paired-end reads and assembled and scaffolded using Dovetail Genomics Hi-C and Chicago long-range contact data. The resulting genome assembly has a total length of 1,901.85 Mb, scaffold N50 length of 273.213 Mb, and includes 5,294 scaffolds. The chromosome-level assembly is composed of 6 macrochromosomes and 11 microchromosomes. A total of 20,764 genes were annotated in the assembly. GC content and gene density are higher for microchromosomes than macrochromosomes, while repeat element distributions show the opposite trend. Pathway analyses provide preliminary evidence that microchromosome and macrochromosome gene content are functionally distinct. Synteny analysis indicates that large microchromosome blocks are conserved among closely related species, whereas macrochromosomes show evidence of frequent fusion and fission events among reptiles, even between closely related species. Conclusions : Our results demonstrate dynamic karyotypic evolution across Reptilia, with frequent inferred splits, fusions, and rearrangements that have resulted in shuffling of chromosomal blocks between macrochromosomes and microchromosomes. Our analyses also provide new evidence for distinct gene content and chromosomal structure between microchromosomes and macrochromosomes within reptiles.
Corresponding Author:	Nazila Koochekian Miami University College of Arts and Science Oxford, OH UNITED STATES
Corresponding Author Secondary Information:	
Corresponding Author's Institution:	Miami University College of Arts and Science
Corresponding Author's Secondary Institution:	
First Author:	Nazila Koochekian
First Author Secondary Information:	
Order of Authors:	Nazila Koochekian Alfredo Ascanio Keaka Farleigh Daren C Card

	Drew R Schield
	Todd A Castoe
	Tereza Jezkova
Order of Authors Secondary Information:	
Response to Reviewers:	Point-By-Point Response to Reviews Reviewer reports: Reviewer #1: I want to thank authors for carefully considering all the comments raised by reviewers. This manuscript will substantially add to the genomic resources for further studies. Most importantly, micro chromosome work will indeed pave way to new research in understanding their nuanced biology and evolution. Great work and congratulations. *** We are pleased that the reviewer was satisfied with our revisions and supportive of the foundational nature of the work on microchromosomes, and we thank them for their time and feedback. Reviewer #2: The authors have done a good job with the revision. I only have a few points that I would like to emphasize and suggest they address further. *** We are happy to hear that the reviewer thought that our previous revision was well done, and thank them for their additional feedback here. 1. In comparison to BUSCO results from other recent squamate genomes (see Figure 2d in https://www.biorxiv.org/content/10.1101/2021.09.28.462146v1.full for a comparison) the BUSCO results from this genome assembly suggest it is not considerably high quality assembly (relatively). The 16% missing and only 64% complete BUSCOs suggest this assembly is relatively incomplete and is a lower quality assembly (more fragmented) than many of the other squamate genomes. This should be explained and discussed in the text, particularly in how this may affect their conclusions about defining the microchromosomes, their synteny analysis, and their pathway analysis. *** In the discussion we now mention the possible effect of the incomplete assembly on our results (lines 234-239, and 284-286) 2. It should be further emphasized throughout that the microchromosome naming designations are putative (and very possibly may not correspond to the karyotype) due to (1) the incomplete nature of the assembly, (2) the splitting of scaffolds into microchromosomes based on bioinformatic predictions, (3) and their naming based on length when some of their lengths are very similar (many less then 200,000 bp difference, Table S1). *** We added this as suggested to the discussion (lines 234-239). 3. Line 181, I think you are missing a number for the upper limit. To define the 14 scaffolds that are > 6mb and < #? *** The upper limit for these 14 scaffolds now been added (75 Mb, line 181). 4. Line 193, I think 'm' is supposed to be a number here. *** The index is explained a couple lines above (line 190). In this case, “m” is a variable based on the species chromosome number.
Additional Information:	
Question	**Response**
Are you submitting this manuscript to a special series or article collection?	No
Experimental design and statistics Full details of the experimental design and statistical methods used should be given in the Methods section, as detailed in our	Yes

Minimum Standards Reporting Checklist. Information essential to interpreting the data presented should be made available in the figure legends. Have you included all the information requested in your manuscript?	
Resources A description of all resources used, including antibodies, cell lines, animals and software tools, with enough information to allow them to be uniquely identified, should be included in the Methods section. Authors are strongly encouraged to cite Research Resource Identifiers (RRIDs) for antibodies, model organisms and tools, where possible. Have you included the information requested as detailed in our Minimum Standards Reporting Checklist?	Yes
Availability of data and materials All datasets and code on which the conclusions of the paper rely must be either included in your submission or deposited in publicly available repositories (where available and ethically appropriate), referencing such data using a unique identifier in the references and in the “Availability of Data and Materials” section of your manuscript. Have you have met the above requirement as detailed in our Minimum Standards Reporting Checklist?	Yes

A chromosome-level genome assembly and annotation of the desert horned lizard, *Phrynosoma platyrhinos,* provides insight into chromosomal rearrangements among reptiles

Running title: genome of *P. platyrhinos*

Nazila Koochekian (*Correspondence): Department of Biology, Miami University, Oxford, OH, 45056, USA. Email: koochen@miamioh.edu

Alfredo Ascanio: Department of Biology, Miami University, Oxford, OH, 45056, USA. Email: ascaniaa@miamioh.edu

Keaka Farleigh: Department of Biology, Miami University, Oxford, OH, 45056, USA. Email: farleik@miamioh.edu

Daren C. Card: Department of Organismic & Evolutionary Biology, Harvard University, Cambridge, MA, 02138, USA, and Museum of Comparative Zoology, Harvard University, Cambridge, MA, 02138, USA. Email: dcard@fas.harvard.edu

Drew R. Schield: Department of Ecology and Evolutionary Biology, University of Colorado, Boulder, CO, 80309, USA. Email: Drew.Schield@colorado.edu

Todd A. Castoe: Department of Biology, University of Texas at Arlington, Arlington, TX, 76019, USA. Email: todd.castoe@uta.edu

Tereza Jezkova: Department of Biology, Miami University, Oxford, OH, 45056, USA. Email: jezkovt@miamioh.edu

ORCIDs:

Nazila Koochekian [0000-0003-4826-098X];

Alfredo Ascanio [0000-0001-9987-7977];

Keaka Farleigh [0000-0002-9195-121X];

Daren C Card [0000-0002-1629-5726];

Drew R Schield [0000-0001-7854-9480];

Todd A Castoe [0000-0002-5912-1574];

Tereza Jezkova [0000-0003-4114-4564];

Abstract

Background. The increasing number of chromosome-level genome assemblies has advanced our knowledge and understanding of macroevolutionary processes. Here, we introduce the genome of the desert horned lizard, *Phrynosoma platyrhinos,* an iguanid lizard occupying extreme desert conditions of the American southwest. We conduct analysis of the chromosomal structure and composition of this species and compare these features across genomes of 12 other reptiles (5 species of lizards, 3 snakes, 3 turtles, and 1 bird).

Findings. The desert horned lizard genome was sequenced using Illumina paired-end reads and assembled and scaffolded using Dovetail Genomics Hi-C and Chicago long-range contact data. The resulting genome assembly has a total length of 1,901.85 Mb, scaffold N50 length of 273.213 Mb, and includes 5,294 scaffolds. The chromosome-level assembly is composed of 6 macrochromosomes and 11 microchromosomes. A total of 20,764 genes were annotated in the assembly. GC content and gene density are higher for microchromosomes than macrochromosomes, while repeat element distributions show the opposite trend. Pathway analyses provide preliminary evidence that microchromosome and macrochromosome gene content are functionally distinct. Synteny analysis indicates that large microchromosome blocks

are conserved among closely related species, whereas macrochromosomes show evidence of frequent fusion and fission events among reptiles, even between closely related species. *Conclusions*: Our results demonstrate dynamic karyotypic evolution across Reptilia, with frequent inferred splits, fusions, and rearrangements that have resulted in shuffling of chromosomal blocks between macrochromosomes and microchromosomes. Our analyses also provide new evidence for distinct gene content and chromosomal structure between microchromosomes and macrochromosomes within reptiles.

Key words: microchromosome; macrochromosome; gene content; synteny; Reptilia

Background

The increasing number of available chromosome-level genome assemblies of non-traditional model organisms has advanced our understanding of genome evolution over large time scales, including intra- and inter-chromosomal rearrangements and karyotype evolution across amniote vertebrates. A major gap in our understanding of amniote genome structure, composition, and evolution has been due to the lack of representative reptilian genomes of high enough quality to compare chromosome composition and structure. From data that is available, reptiles (the clade of Sauropsida) appear to exhibit particularly high levels of karyotypic variation (Fig. 1)[1, 2]. Much of this karyotypic variation is apparently due to frequent merging, splitting, and rearrangements among chromosomes, resulting in varying numbers and sizes of chromosomes even among closely related taxa (Fig. 1). Unlike mammalian genomes which lack microchromosomes, most reptilian genomes contain both macrochromosomes and microchromosomes [3]. The condition of possessing both macro- and microchromosomes appears to represent an ancient ancestral state that spans 400–450 million years of evolutionary history, as microchromosomes are present in many ancient chordates, fish, and amphibians, and all amniote vertebrates except mammals and crocodilians [3].

Microchromosomes are generally identified by their smaller size (50 Mb threshold in squamates [4]). In the chicken, for example, microchromosomes range from 3.5 to 23 Mb [5], compared to macrochromosomes which range from 40 to 250 Mb [6].

Although microchromosome organization in avian species is relatively conserved at a karyotypic level [7], microchromosomes of non-avian reptiles vary considerably in number and size [8,9], potentially due to relatively high recombination rates [10] that lead to higher rates of chromosomal rearrangement [3,11]. Despite being a promising system in which to study karyotypic evolution, relatively little is known about the genomic features of macrochromosomes and microchromosomes and how these features evolve across Reptilia [12]. Moreover, microchromosomes appear structurally and functionally distinct from macrochromosomes [13], and a deeper characterization of these distinctions may improve our understanding of the functional and evolutionary significance of the presence/absence of microchromosomes, and the presence of genes on micro- versus macrochromosomes. Despite interest in the processes and patterns related to chromosome evolution in reptiles, progress has been limited by the availability of relatively few high-quality reptile genomes available for comparative study. In lizards, only five genomes are annotated and assembled at the level of chromosomes (i.e., chromosome-size scaffolds that in many cases have been ascribed to specific chromosomes): the green anole, *Anolis carolinensis* with 6 chromosomes and 7 microchromosomal linkage groups [14], the viviparous lizard, *Zootoca vivipara* with 19 chromosomal linkage groups [15], the sand lizard, *Lacerta agilis* with 18 autosomes and Z and W sex chromosomes [16], the common wall lizard, *Podarcis muralis* with 18 autosomes and a Z sex chromosome [17], and the Argentine black and white tegu, *Salvator merianae*, with chromosome-scale scaffolds that have not been fully ascribed to specific chromosomes [18].

Here we present a new chromosome-level genome assembly of the desert horned lizard (*P. platyrhinos*; NCBI:txid52577) and use this genome to conduct comparative analysis of chromosome content and evolution across reptiles. This species is widely distributed across the

southwestern deserts of north America, including some of the hottest and driest places on Earth (e.g. Death valley in the Mojave Desert; [19]) which makes it an attractive model organism to study adaptation to extreme thermal environments. We have annotated the genome assembly and assessed large-scale structure and composition of the genome across macrochromosomes and microchromosomes. Using this new resource, we conduct synteny analyses to explore major changes in genome organization by making comparisons with existing chromosome-level annotated genomes of other lizards (*A. carolinensis, S. merianae, L. agilis, Z. vivipara* and *P. muralis*), snakes (*Crotalus viridis* [20], *Thamnophis elegans* [21], and *Naja naja* [22]), a bird (*Gallus gallus* [23]), and turtles (*Trachemys scripta* [24], *Gopherus evgoodei* [25], and *Dermochelys coriacea* [9]). Our findings reveal differences in structure and gene content of macrochromosomes and microchromosomes in *P. platyrhinos* and highlight numerous chromosomal rearrangements among reptiles.

Analysis

Genome assembly, transcriptome assembly, and chromosome identification

The genome of *P. platyrhinos* was sequenced at 21,053.74-fold physical coverage using the Dovetail Genomics HiRise™ [26] sequencing and assembly approach that combines a contig-level assembly produced from shotgun Illumina sequencing with long-range scaffolding data from Chicago and Hi-C library preparations (Table 1). The final assembly included 5,294 total scaffolds, with 7 large scaffolds and 10 smaller scaffolds comprising 99.56% of the genome assembly. The known karyotype of the species is composed of 6 macrochromosomes and 11 microchromosomes [27,28] and we assumed this karyotype when linking chromosomes to their representative assembly scaffolds. Using chromosome-linked gene markers from *A. carolinensis* and *Leiolepis reevesii* [29], the 7 largest scaffolds were assigned to macrochromosomes 1-6 (two scaffolds corresponded to the two arms of macrochromosome 3;

Table S1 and Table S2). Ten smaller scaffolds were assigned to microchromosomes, and one of these scaffolds was manually split into two microchromosomes (Table S1). We followed previous studies [8] to infer the location of the putative split between chromosomes by combining evidence from physically-linked Chicago scaffolds that cannot span multiple chromosomes, repeat element and GC composition, and synteny with chromosomes of other species (see Methods).

The chromosome-linked gene markers used to identify chromosome scaffolds do not identify specific microchromosome numbers (Table S2), so we ordered the assembled *P. platyrhinos* microchromosomes by descending length and numbered them microchromosomes 1-11 (Table S1). Sex chromosomes are conserved across iguanid lizards [30] and we identified microchromosome 9 as the X chromosome in *P. platyrhinos* based on homology with X-linked markers in *A. carolinensis* (*ATP2A2*, *FZD10*, and *TMEM132D* [30]; Table S2).

RNA-sequencing of 8 tissues (liver, lungs, brain, muscle, testes, heart, eyes, and kidneys) was used to assemble the transcriptome of *P. platyrhinos* using Trinity r2014 0413p1 [31]. The final transcriptome assembly contained 199,541 transcripts comprising 199,500 Trinity-annotated genes, with an average length of 1,438 base pairs and an N50 length of 2,420 bp.

Genome annotation and chromosomal composition

We annotated 20,764 protein-coding genes in the *P. platyrhinos* genome assembly (JAIPUX010000000) using the gene prediction software MAKER v. 2.31.10 [32] and gene predictions based on AUGUSTUS v. 3.2.3. [33]. Among the total annotated genes, 16,384 genes were identified using searches against protein sequences in databases NCBI and Interpro [34]. We identified 4,324 complete and fragmented BUSCO markers in the *P. platyrhinos* genome annotation from the total 5,310 BUSCO markers present in the library "tetrapoda_odb10.2019-11-20" (Table 2). Our repeat annotation identified 44.45% of the

147 genome as repetitive elements (Table S3) using RepeatModeler v. 1.0.11 [35] and
148 RepeatMasker v. 4.0.8 [36]. The major components of the genomic repeat content included
149 simple sequence repeats (6.90%), as well as L2/CR1/Rex (6.88%), hobo-Activator (5.98%), and
150 Tourist/Harbinger (4.90%) transposable element families (Table S3).

151 Chromosomal composition analyses indicate that overall gene density (GD) and GC-
152 content tended to be lower on *P. platyrhinos* macrochromosomes (mean ± sd GD = 0.19 ± 0.14,
153 median = 0.17 per Mb; mean ± sd GC% = 35.9 ± 1.2%, median = 35.9%) than
154 microchromosomes (mean ± sd GD = 0.27 ± 0.16, median = 0.29 per Mb; mean ± sd GC% =
155 38.5 ± 2.8%, median = 38.2%; Fig. 2 and S1). Conversely, repeat elements density tended to
156 be higher on macrochromosomes (mean ± sd = 44.6 ± 5.6%, median = 43.3% per Mb) than
157 microchromosomes (mean = 39.4 ± 10%, median = 38.1% per Mb; Fig. 2 and S1). These
158 differences in GD, GC-content, and repeat elements between macro and microchromosomes
159 were statistically significant (Wilcoxon-W = 137011, p-value = $5.7*10^{-16}$ for GD; Wilcoxon-W =
160 68322, p-value < $2.2*10^{-16}$ for GC-content; and Wilcoxon-W = 283330, p-value < $2.2*10^{-16}$ for
161 repeat elements).

162 ***Pathway analysis***

163 We assessed whether macrochromosomes and microchromosomes contain distinct
164 functional classes of genes using pathway analyses. From the total of 16,384 protein coding
165 genes that were identified by homology search, 9,590 gene IDs on macrochromosomes and
166 3,129 on microchromosomes were identifiable by PANTHER16.0 [37,38] using the protein
167 family/subfamily library (Fig. S2). These genes were classified into a total of 164 pathways from
168 about 177 available pathways in PANTHER. The highest number of genes belonged to the
169 “Wnt signaling pathway (P00057)” and “Gonadotropin-releasing hormone receptor pathway
170 (P06664)”, which together accounted for more than 10% (more than 5% each) of the

macrochromosomal and microchromosomal genes. We compared the frequencies of genes in each PANTHER pathway between macrochromosomes and microchromosomes and found 37 pathways where all genes were located on macrochromosomes (Table S4), with 13 pathways having all genes localized to a single macrochromosome. Among microchromosomes, we found that three pathways have genes exclusively found on only microchromosomes and in all three pathways, these genes were located on a single microchromosome (Table S4). These 40 pathways (37 for macrochromosomes + 3 for microchromosomes) mostly belong to biosynthesis, signaling, metabolism, and degradation pathways (in descending order).

Synteny analysis

We investigated how reptilian genome composition has been impacted by chromosomal rearrangements through evolutionary time using comparative synteny analyses among reptiles. We conducted pairwise analyses of synteny between the *P. platyrhinos* genome and 12 species (five lizards, three snakes, three turtles, and a bird) for which chromosome-level genome assemblies were available (Fig. 3)[25]. The genome of *S. merianae* has not been assembled to chromosomes but the karyotype of this species is known (5 macrochromosome and 14 microchromosomes; [39]) so in this study we used 19 largest scaffolds from the *S. merianae* assembly with 5 scaffolds > 200 Mb, and 75 Mb > 14 scaffolds > 6 Mb). We performed synteny analyses using a 'chromosome painting' technique (see Methods), which established homology between sets of 100 bp *in silico* 'markers' from the *P. platyrhinos* chromosome scaffolds and regions of the genomes of the other reptile species (Table S5). We quantitatively assessed the degree to which syntenic blocks from each *P. platyrhinos* chromosome scaffold are dispersed across chromosomes of the other species (Fig. 4) using a dominance analysis [40], more commonly used in ecological community assessments. Specifically, dispersion was measured using the Simpson's Dominance Index reciprocal (SR), with which we consider an effective number of target chromosomes in other species onto which the homologies of a given *P.*

196 *platyrhinos* chromosome appear*.* This index ranges from 1 to *m*, where *m* is the number of
197 chromosomes of the target species being compared to *P. platyrhinos*. A value of 1 represents
198 high dominance, which in this context indicates that syntenic blocks from a chromosome of *P.*
199 *platyrhinos* are restricted to a single chromosome of another species. A value of *m* would mean
200 all chromosomes of the target species contain an even proportion of *P. platyrhinos* syntenic
201 blocks. If a large syntenic block is retained in one chromosome while a few proportionally small
202 syntenic blocks are distributed across other target chromosomes, the resulting dominance value
203 will trend toward 1.
204 Our results show that macrochromosomes tend to have a higher degree of dispersion
205 across different chromosomes of other species than microchromosomes (e.g.,
206 macrochromosome 1 SR = 2.38 ± 0.96; microchromosome 1 SR = 1.45 ± 0.45), except for
207 macrochromosome 6 (SR = 1.44 ± 0.27; Fig. 5a). However, this chromosomal rearrangement
208 does not follow the same pattern across species (Fig. 4). For example, *A. carolinensis* shows
209 the highest values for SR in microchromosomes (Fig. 5b), but this may be an artifact of this
210 species having an incomplete genome assembly for microchromosomes. In other lizards and
211 snakes (with the exception of *C. viridis*), SR ~ 1 for all microchromosomes (except
212 microchromosome 6). In *G. gallus*, SR ~ 1 for all microchromosomes except microchromosome
213 1. In turtles, mean SR values for microchromosomes are > 1, but this is largely driven by higher
214 SR values on microchromosomes 1, 4, and 6 (Fig. 4).
215 Macrochromosome synteny appears highly conserved between *P. platyrhinos* and *S.*
216 *merianae*. Among the closest relatives of *P. platyrhinos*, *A. carolinensis* has the same
217 macrochromosome arrangement as *P. platyrhinos* (Figs. 3-5). In the more distantly related
218 snakes, *N. naja* and *C. viridis*, however, macrochromosomes 3 and 5 show high SR values and
219 the remaining macrochromosomes have SR ~ 1. Compared to the other snakes, *T. elegans*
220 (along with lizards in the family Lacertidae) generally possess a greater number of smaller
221 macrochromosomes than *P. platyrhinos* and associated higher SR values. At greater

phylogenetic distances, the breakdown of chromosomal synteny from lizards to other reptilian lineages becomes more apparent (cumulative SR ~ 30 in turtles) and showing greater rearrangements and partitions of syntenic blocks in macrochromosomes than in microchromosomes (Fig. 4 and 5b).

Our results also show that rearrangements between macro- and microchromosomes are apparently common throughout the evolution of Reptilia, including macro and microchromosomes fusing together to form single macrochromosomes. For example, microchromosomes 5 and 6 in *P. platyrhinos* form a macrochromosome in *L. agilis, Z. vivipara*, and *P. muralis*, chromosome 6 of *P. platyrhinos* is syntenic with a macrochromosome and a microchromosome in *S. merianae,* and microchromosome 6 of *P. platyrhinos* comprises two microchromosomes in *S. merianae*, *G. gallus,* and turtle species (Fig. 3).

Discussion

The *P. platyrhinos* genome is only the second chromosome-level assembly available for the diverse lizard family Iguanidae (after *A. carolinensis*), and the only member of this family with well assembled microchromosomes, thereby contributing a new valuable resource for comparative genomics of reptiles. For *P. platyrhinos*, we identified scaffolds representing the 6 macrochromosomes and 11 microchromosomes that comprise the known karyotype for the genus *Phrynosoma* [27,28,41]. We note that the chromosome number designations especially for microchromosomes, however, may differ from that of the known karyotype due to multiple factors, including the lack of chromosome linked markers for individual microchromosomes, our post-hoc bioinformatic-driven inferences of microchromosome boundaries, and the completeness of our genome assembly potentially impacting the accuracy of estimates of the true relative sizes (and size differences) of all microchromosomes. Despite this, the higher contiguity and completeness of microchromosomal scaffolds in the *P. platyrhinos* genome

relative to that of *A. carolinensis* does enable some of the first comparisons of chromosome evolution in lizards that incorporates patterns distinct to macro- versus microchromosomes. Our analyses of this and other comparative reptilian genomes highlight distinct functional classes of genes, chromosomal structure, and rearrangement patterns in microchromosomes compared to macrochromosomes.

Consistent with previous studies of reptilian chromosome composition [8,10,42], we find that in *P. platyrhinos*, GC content, gene density, and repeat element density differ between macrochromosomes and microchromosomes, with gene density and GC content being higher on microchromosomes and repeat elements being more densely distributed on macrochromosomes. Patterns of high gene density on microchromosomes have been hypothesized to be an evolutionary solution to reduce overall DNA mass and increase recombination rates between coding regions, predominantly by reducing repeat element content [3]. High recombination rates further increase GC content due to GC-biased gene conversion [43], leading to a higher frequency of GC bases on microchromosomes that can house functionally different gene content compared to macrochromosomes [13], a pattern we also observed in the *P. platyrhinos* genome (Fig. 2 and S1).

Our synteny analyses across reptile genomes revealed that splitting, fusion, and rearrangement events among chromosomes have occurred frequently and repeatedly throughout reptile evolution. This pattern of chromosome blocks shifting between macro-, and microchromosome-linkage likely explains some unusual patterns of gene density, GC-content, and repeat elements, such as blocks of high gene density on a macrochromosome that may represent ancestral fragments derived from microchromosomes. For example, high GC content and gene density relative to other macrochromosomes on one end of macrochromosome 6 of *P. platyrhinos* (extending for ~40 Mbp; Fig. 2) supports the scenario that a microchromosomal region with higher gene and GC density was recently translocated to a macrochromosome in the ancestor of *P. platyrhinos*. This process may have also contributed to the observed variation

in the numbers and sizes of macro- and microchromosomes, even among closely related species (e.g., *P. platyrhinos* versus *A. carolinensis*, and *C. viridis* versus *T. elegans*). Among macrochromosomes, fusion, splitting, and translocation to other chromosomes in more distantly related species such as turtles and chicken are common, whereas microchromosomes of *P. platyrhinos* typically remain in single homologous blocks in these other reptilian lineages, though there seem to be exceptions based on our analysis (Fig. 4 and Fig. 5b). Broadly, these findings suggest that ancestral chromosomal rearrangements may have resulted in regions of reptilian genomes that have not yet reached mutational and compositional equilibria, which are otherwise characteristic of macro- and microchromosomal regions, following ancestral chromosomal rearrangement events.

Adding to the growing body of evidence for the structural, compositional, and evolutionary distinctions between micro- and macrochromosomes [10,13,44,45,46,47,48], our analyses suggest that the gene content of these two classes of chromosomes may be distinct in function. Our preliminary observation of enrichment of genes from certain pathways on individual chromosomes or on macro- and microchromosomes more generally warrants further investigation. These biases could be driven by ancestral contingencies of gene content or active translocations of genes across chromosome classes, which may suggest a functionally driven basis for such biases. Our results, however, need to be interpreted with caution because these pathways are incomplete. Many genes are still functionally unknown, and our genome assembly is partially fragmented and missing some expected genes in Tetrapoda (Table 2). Nevertheless, our inferences, together with other emerging evidence for the compositional and functional distinctiveness between micro- and macrochromosomes [10,13,44] suggest that there may be key functional, evolutionary, and mechanistic features that distinguish these chromosome classes that explain the significance of the presence and abundance of microchromosomes across eukaryote lineages.

Methods

Genome and transcriptome assembly

We sequenced and assembled the reference genome from a female desert horned lizard collected in Dry Lake Valley, Nevada (NCBI accession SAMN17187150). This specimen was collected and euthanized according to Miami University Institutional Animal Care and Use Committee protocol 992_2021_Apr. Liver tissue was snap frozen in liquid nitrogen and sent to Dovetail Genomics (Scotts Valley, CL) for extraction of DNA and construction of shotgun, Chicago, and Dovetail Hi-C paired end libraries. DNA was extracted using buffer G2, and Qiagen protease. Three initial shotgun sequencing libraries were constructed by fragmenting DNA extracts to 475 bp and using a TruSeq PCR-free library prep kit to ligate sequencing adapters and amplify each library. The resulting libraries were sequenced on an Illumina HiSeqX (Illumina HiSeq X Ten, RRID:SCR_016385) and resulted in 859.9 million read pairs from paired end libraries (totaling 246 Gbp; see Table 3 for the number of sequenced reads for each library). Reads were trimmed for quality, sequencing adapters, and mate pair adapters using Trimmomatic (Trimmomatic, RRID:SCR_011848) [49], Using these data, contigs and small scaffolds were assembled using Meraculous 2.2.4 (diploid_mode 1; RRID:SCR_010700) [50] with a kmer size of 49-mers. which produced an assembly with a scaffold N50 of 0.013 Mb.

The original assembly was first scaffolded using a Chicago library according to the manufacturer's protocol. Three Chicago libraries were prepared as described previously [26]. Briefly, for each library, ~500ng of HMW gDNA was reconstituted into chromatin *in vitro* and fixed with formaldehyde. Fixed chromatin was digested with DpnII, the 5' overhangs filled in with biotinylated nucleotides, and then free blunt ends were ligated. After ligation, crosslinks were reversed, and the DNA purified from protein. Purified DNA was treated to remove biotin that was not internal to ligated fragments. The DNA was then sheared to ~350 bp mean fragment size and sequencing

libraries were generated using NEBNext Ultra enzymes and Illumina-compatible adapters. Biotin-containing fragments were isolated using streptavidin beads before PCR enrichment of each library. The libraries were sequenced on an Illumina HiSeqX. The number and length of read pairs produced for all libraries was 528 million 2x150 bp paired end reads (see Table 3 for the number of sequenced reads for each library). The resulting scaffolded assembly was far more contiguous with a scaffold N50 of 63.431 Mb. Lastly, a final round of scaffolding was performed using data from the Dovetail Hi-C library according to the manufacturer's protocols. Three Dovetail Hi-C libraries were prepared in a similar manner as described previously [51]. Briefly, for each library, chromatin was fixed in place with formaldehyde in the nucleus and then extracted. The following steps were the same as creating Chicago libraries. The number and length of read pairs produced for all libraries was 515 million 2x150 bp paired end reads (see Table 3 for the number of sequenced reads for each library). The input *de novo* assembly, Chicago library reads, and Dovetail Hi-C library reads were used as input data for HiRise [52], a software pipeline designed specifically for using proximity ligation data to scaffold genome assemblies. First, Chicago library sequences were aligned to the draft input assembly using SNAP v1.0.0 [53]. The separations of Chicago read pairs mapped within draft scaffolds were analyzed by HiRise to produce a likelihood model for genomic distance between read pairs, and the model was used to identify and break putative misjoins, to score prospective joins, and make joins above a threshold. After aligning and scaffolding Chicago data, Dovetail Hi-C library sequences were aligned and scaffolded following the same method. The final assembly (NCBI accession PRJNA685451) has a length of 1,901.85 Mb with a contig N50 of 12.04 kb and a scaffold N50 of 273.213 Mb (see Table 1 for more statistics for this genome assembly).

Transcriptomic libraries were sequenced from 8 tissues (liver, lungs, brain, muscle, testes, heart, eyes, and kidneys) from a male lizard collected and euthanized according to Miami University Institutional Animal Care and Use Committee protocol 992_2021_Apr at the same locality as the genome animal. For each library, total RNA was extracted using Trizol reagent,

and unstranded mRNAseq libraries were individually prepared using an NEBNext Ultra RNA Library Prep kit with library insert sizes of 250-300 bp and sequenced on an Illumina Hiseq4000 platform (Illumina HiSeq 4000 System, RRID:SCR_016386) using a paired-end 150 bp run by Novogene Corporation Inc (Table 4). We used Trinity r2014 0413p1 to assemble transcriptome reads from all tissues (using min_kmer_cov:1 and default settings).

Chromosome identification

According to the karyotype for phrynosomatid [41] and *P. platyrhinos* [27,54] (2n=34), we expected 6 pairs of macrochromosomes and 11 pairs of microchromosomes (one pair of microchromosomes is expected to be sex linked) for *P. platyrhinos*, and assumed this karyotype was correct for organizing our scaffolded genome assembly. Assigning scaffolds to specific chromosomes was done using blast+2.8.0 [55] using program "blastx" (options "num_threads"=4, "-max_target_seqs"=10, "-evalue"= 1e-5, and "-outfmt"=11). We used chromosome-linked gene markers in other close species (*A. carolinensis*, *Leiolepis reevesii*) [29] and X-linked markers in *A. carolinensis* [39] downloaded from NCBI (Table S1) to identify the genomic location of each gene marker. Available markers for macrochromosomes in lizards were matched to seven of the largest scaffolds (two scaffolds for chromosome 3), which we sorted by size and named macrochromosomes 1-6. From the remaining scaffolds, 10 scaffolds (> 8 Mbp) were selected as potential microchromosomes. This suggested that one scaffold comprises two microchromosomes fused together as the expected number of microchromosomes was 11. Synteny analysis suggested that scaffold "Scf4326_4427" (Fig. 6) has at least three origins in other closely related species. For example, in *S. merianae,* three microchromosome account for this scaffold, while the rest of scaffolds were linked to a specific microchromosome. Given that Chicago libraries reconstitute chromatin *in vitro*, interactions between distinct chromosomes are significantly reduced compared to *in vivo* Hi-C libraries [56]. Also, microchromosomes may have a greater frequency of inter-chromosomal contact [12] than

expected in models used to scaffold based on Hi-C sequencing data. Therefore, we scanned for breakpoints between Chicago scaffolds in microchromosome scaffolds and for each of these breakpoints, we used multiple forms of evidence to assess whether a scaffold should be manually split. Following Schield [8], patterns of GC content, repeat density, and gene density at each breakpoint were assessed and we looked for instances in which there were abrupt shifts in these measures near breakpoints between Chicago scaffolds. At two of these breakpoints on the putatively artificially-merged (with a window of about 100 bp Ns/gaps) scaffold "Scf4326_4427", we observed elevated GC content, and reduced repeat elements density (Fig. S3). Based on these patterns, we chose to split this scaffold at the breakpoint location with reduced gene density to produce a final, curated assembly with the expected number of microchromosomes and finally numbered them based on their size.

Genome annotation

Repeat elements were first identified using RepeatModeler v. 1.0.11 (RepeatModeler, RRID:SCR_015027) [35] for *de novo* prediction of repeat families. To annotate genome-wide complex repeats, we used RepeatMasker v. 4.0.8 (RepeatMasker, RRID:SCR_012954) [36] with default settings to identify known Tetrapoda repeats present in the curated Repbase database release 20181026 [57]. We then ran 2 iterative rounds of RepeatMasker to annotate the known and the unknown elements identified by RepeatModeler, respectively, where the genome sequence provided for each analysis was masked based on all previous rounds of RepeatMasker.

We used MAKER v. 2.31.10 [32] as a consensus-based approach to annotate protein-coding genes in an iterative fashion. For annotation, a genome with complex, interspersed repeats hard masked as Ns was supplied and we set the 'model_org' option to 'simple' in the MAKER control file (maker_opts.ctl) to have MAKER soft mask simple repeats prior to gene annotation. The full *de novo P. platyrhinos* transcriptome assembly and protein datasets consisting of all annotated

proteins for *A. carolinensis* [14] from NCBI were used as the evidence for protein coding gene prediction. For the first round of annotation, “est2genome” and “protein2genome” were set to 1 to predict genes based on the aligned transcripts and proteins. Using the gene models from the first round of MAKER, we were able to train gene prediction software AUGUSTUS v. 3.2.3. (Augustus, RRID:SCR_008417) [33]. To do so, we used Benchmarking Universal Single-Copy Orthologs (BUSCOs) v. 2.0.1 (BUSCO, RRID:SCR_015008), which has an internal pipeline to automate the training of Augustus based on a set of conserved, single-copy orthologs for Tetrapoda (Tetrapoda odb9 dataset) [58]. We ran BUSCO in the ‘genome’ mode and specified the ‘--long' option to have BUSCO perform internal Augustus parameter optimization. Then we ran MAKER with *ab initio* gene prediction (‘est2genome=0’ and ‘protein2genome=0’ options set) using transcripts, proteins, and repeat elements resulted from the first MAKER round as the empirical evidence (in GFF format) to produce gene models using the AUGUSTUS within the MAKER. For all MAKER analyses, we used default settings, except for ‘trna’ (set to 1), ‘max_dna_len’ (set to 300,000) and ‘split_hit’ (set to 20,000). We used the gene models from our second round of MAKER annotation to re-optimize AUGUSTUS as described above before running one final MAKER analysis (round 3) with the re-optimized AUGUSTUS settings (all other settings are identical to round 2). We compared Annotation Edit Distance (AED) distributions, gene numbers, and average gene lengths across each round of Maker annotation to assess quality and used our final MAKER round (round 3; N = 20,764 genes) as our final gene annotation.

We ascribed gene IDs based on homology using reciprocal best-blast (with e-value thresholds of 1e-5) and stringent one-way blast (with an e-value threshold of 1e-8) searches against protein sequences from NCBI for *A. carolinensis*, *Pogona vitticeps* [59]*, P. muralis* [17], *Gekko Japanese* [60], *Python molurus* [61], *Pseudonaja textilis* [62], *Notechis scutatus* [62], *Protobothrops mucrosquamatus* [63]*, Thamnophis sirtalis* [64]*, Alligator mississippiensis* [65]*, Alligator sinensis* [66,67]*, Crocodylus porosus* [68]*, Chrysemys picta* [69]*, Terrapene carolina*

[70], *Chelonia mydas* [71], *Pelodiscus sinensis* [71], *G. gallus, Homo sapiens* [72], *Mus musculus* [73], and Swiss-Prot [74] using a custom reciprocal best blast (RBB) script (orthorbb 2.2) [75]. We also searched our annotated transcriptome against Interpro database via Interproscan--5.36-75.0 [76].

Pathway analysis

To compare macrochromosomes and microchromosomes functionally, protein coding genes on each chromosome were analyzed using gene IDs resulted from homology search. An ID list of all annotated genes on each chromosome was used for pathway analysis in PANTHER16.0 (via browser and "Gene List Analysis" tools option) classification system. Four model organisms (*A. carolinensis*, *G. gallus, M. musculus,* and *H. sapiens*) were selected as the reference for gene IDs. PANTHER assigned each gene to at least one of the 164 pathways identified for *P. platyrhinos* genome annotation (with a range from 2 to 759 genes in each pathway; Fig. S4). The distributions of each pathway among different chromosomes were compared using pathway results for each chromosome to identify potential pathways that belong to a specific chromosome/group of chromosomes.

Synteny and chromosomal composition

We used a python script ‘‘slidingwindow_gc_content.py" [77] to estimate GC content genome wide in windows of 1 Mbp. We estimated gene and repeat elements densities for the final genome assembly using python script "window_quantify.py" with a window size of 1 Mbp. As the distribution of these variables (GD, GC-content, repeated elements) was highly skewed/non-normal, we performed Wilcoxon rank sum tests to check for statistically significant differences between macro and microchromosomes.

We explored broad-scale structural evolution across reptilian genomes using synteny analyses. We obtained chromosome-level genome assemblies from NCBI database for five lizards (*A. carolinensis* (GCA_000090745.2)*, S. merianae* (GCA_003586115.2)*, L. agilis* (GCA_009819535.1)*, P. muralis* (GCA_004329235.1)*,* and *Z. vivipara* (GCA_011800845.1)), three snakes (*C. viridis* (GCA_003400415.2), *T. elegans* (GCA_009769535.1), and *N. naja* (GCA_009733165.1)), one bird (*G. gallus* (GCA_000002315.5)), and three turtles (*T. scripta* (GCA_013100865.1), *G. evgoodei* (GCA_007399415.1), and *D. coriacea* (GCA_009764565.3)). We used a previously established method for in silico painting [44,78] to partition the *P. platyrhinos* genome to 18.39 million 100-bp markers. As input for this approach, we used blast+2.9.0 to blast the markers against each genome (with "blastn" program and setting "-max_hsps" and "-max_target_seqs" to 1, "outfmt"=6 qseqid sseqid sstart length pident, "num_threads"=3, and the rest as default). Following Schield et al. (2019), homology signals for chromosome painting had two main conditions: 1) each marker should have an alignment length of 50 bp or greater, and 2) at least five consecutive markers must be present to infer homology (Table S5). This was determined for scaffolds from each species. For posterior analyses based on the synteny results, only the assembled chromosomes of each species (based on the reference assembly) were considered. *Salvator merianae* was the only species in our analysis without assembled chromosomes, so we analyzed the 19 longest scaffolds (since karyotype analysis showed 2n=38) containing the majority of confirmed markers [39].

To assess the distribution of syntenic blocks of *P. platyrhinos* across scaffolds from the 12 target species, we calculated Simpson's Dominance Index (D) and its reciprocal, which, in this context, can be considered the effective number of target chromosomes (C) containing homologies from a given *P. platyrhinos* chromosome:

$$D_{ij} = \sum_{k=1}^{m} p_{ijk}^2$$

$$C_{ij} = \frac{1}{D_{ij}}$$

Where i represents a *P. platyrhinos* chromosome, j represents a target species, m is the number of scaffolds in the target species j containing homologies from the i^{th} *P. platyrhinos* chromosome, and k represents a specific target scaffold. Values of D can range between 0 (low dominance, i.e., high spread of homologies) and 1 (full dominance, i.e., homologies remained in one target scaffold). Values of C can range between 1 (full dominance) and m (low dominance, i.e., equal spread of the i^{th} homologies across m target scaffolds).

Data Availability

The chromosome-level genome assembly, annotation files, and other supporting data sets are available in the *GigaScience* database (GigaDB) [79]. Raw genomic and transcriptomic sequencing reads, and genome assembly and annotation were deposited in the NCBI under BioProject number PRJNA685451.

List of abbreviations

AED: Annotation Edit Distance

BUSCO: Benchmarking Universal Single-Copy Orthologs

C: Effective number of target Chromosomes

D: Simpson's Dominance index

GD: Gene Density

SR: Simpson's Reciprocal

Ethics Approval

All animal collected and euthanized according to Miami University Institutional Animal Care and Use Committee protocol 992_2021_Apr.

Competing interests

The authors declare that they have no competing interests.

Authors' contributions

N.K. and T.J. designed the project and wrote the first draft of the manuscript. N.K., A.A., K.F., D.C.C., and D.R.S. performed bioinformatics and data analyses. All authors contributed to writing and approved the final manuscript.

Acknowledgments

This work was supported by startup funds from Miami University to T. Jezkova. K. Farleigh was supported by the National Science Foundation Graduate Research Fellowship Program (Award # 2037786). We thank Aaron Ambos and Dr. Jef Jaeger for help with obtaining specimens. The analyses were performed on Miami University Redhawk cluster with incredible assistance from Dr. Jens Mueller.

References

1. Deakin, J. E., and Ezaz, T. (2019). Understanding the Evolution of Reptile Chromosomes through Applications of Combined Cytogenetics and Genomics Approaches. *Cytogenetic and Genome Research*, *157*, 7–20. https://doi.org/10.1159/000495974

2. Gemmell, N. J., Rutherford, K., Prost, S., Tollis, M., Winter, D., Macey, J. R., Adelson, D. L., Suh, A., Bertozzi, T., Grau, J. H., Organ, C., Gardner, P. P., Muffato, M., Patricio, M., Billis, K., Martin, F. J., Flicek, P., Petersen, B., Kang, L., … Stone, C. (2020). The tuatara genome reveals ancient features of amniote evolution. *Nature*, *584*, 403–409. https://doi.org/10.1038/s41586-020-2561-9

3. Burt, D. W. (2002). Origin and evolution of avian microchromosomes. *Cytogenetic and Genome Research*, *96*, 97–112. https://doi.org/10.1159/000063018

4. Waters, P. D., Patel, H. R., Ruiz-herrera, A., Alvarez-Gonzalez, L., Lister, N. C., Simakov, O., Ezaz, T., Kaur, P., Frere, C., Grützner, F., Georges, A., and Graves, J. A. M. (2021). *Microchromosomes are building blocks of bird , reptile and mammal chromosomes*.

5. Solinhac, R., Leroux, S., Galkina, S., Chazara, O., Feve, K., Vignoles, F., Morisson, M., Derjusheva, S., Bed'hom, B., Vignal, A., Fillon, V., and Pitel, F. (2010). Integrative mapping analysis of chicken microchromosome 16 organization. *BMC Genomics*, *11*, 616. https://doi.org/10.1186/1471-2164-11-616

6. Axelsson, E. (2005). Comparison of the chicken and turkey genomes reveals a higher rate of nucleotide divergence on microchromosomes than macrochromosomes. *Genome Research*, *15*, 120–125. https://doi.org/10.1101/gr.3021305

7. O'Connor, R. E., Kiazim, L., Skinner, B., Fonseka, G., Joseph, S., Jennings, R., Larkin, D. M., and Griffin, D. K. (2019). Patterns of microchromosome organization remain highly

conserved throughout avian evolution. *Chromosoma*, *128*, 21–29. https://doi.org/10.1007/s00412-018-0685-6

8. Schield, D. R., Card, D. C., Hales, N. R., Perry, B. W., Pasquesi, G. M., Blackmon, H., Adams, R. H., Corbin, A. B., Smith, C. F., Ramesh, B., Demuth, J. P., Betrán, E., Tollis, M., Meik, J. M., Mackessy, S. P., and Castoe, T. A. (2019). The origins and evolution of chromosomes, dosage compensation, and mechanisms underlying venom regulation in snakes. *Genome Research*, *29*, 590–601. https://doi.org/10.1101/gr.240952.118

9. Bentley, B., Komoroske, L., and Mazzoni, C. (2021). Leatherback turtle genome. *BioRxiv*.

10. Schield, D. R., Pasquesi, G. I. M., Perry, B. W., Adams, R. H., Nikolakis, Z. L., Westfall, A. K., Orton, R. W., Meik, J. M., Mackessy, S. P., and Castoe, T. A. (2020). Snake Recombination Landscapes Are Concentrated in Functional Regions despite PRDM9. *Molecular Biology and Evolution*, *37*, 1272–1294. https://doi.org/10.1093/molbev/msaa003

11. Damas, J., Kim, J., Farré, M., Griffin, D. K., and Larkin, D. M. (2018). Reconstruction of avian ancestral karyotypes reveals differences in the evolutionary history of macro- and microchromosomes. *Genome Biology*, *19*, 155. https://doi.org/10.1186/s13059-018-1544-8

12. Axelsson, E., Webster, M. T., Smith, N. G. C., Burt, D. W., and Ellegren, H. (2005). Comparison of the chicken and turkey genomes reveals a higher rate of nucleotide divergence on microchromosomes than macrochromosomes. *Genome Research*, *15*, 120–125. https://doi.org/10.1101/gr.3021305

13. Perry, B. W., Schield, D. R., Adams, R. H., and Castoe, T. A. (2020). Microchromosomes Exhibit Distinct Features of Vertebrate Chromosome Structure and Function with Underappreciated Ramifications for Genome Evolution. *Molecular Biology and Evolution*, 1–7. https://doi.org/10.1093/molbev/msaa253

14. Alföldi, J., Di Palma, F., Grabherr, M., Williams, C., Kong, L., Mauceli, E., Russell, P., Lowe, C. B., Glor, R. E., Jaffe, J. D., Ray, D. A., Boissinot, S., Shedlock, A. M., Botka, C., Castoe, T. A., Colbourne, J. K., Fujita, M. K., Moreno, R. G., ten Hallers, B. F., … Lindblad-Toh, K. (2011). The genome of the green anole lizard and a comparative analysis with birds and mammals. *Nature*, *477*, 587–591. https://doi.org/10.1038/nature10390

15. Yurchenko, A. A., Recknagel, H., and Elmer, K. R. (2020). Chromosome-level assembly of the common lizard (Zootoca vivipara) genome. *Genome Biology and Evolution*. https://doi.org/10.1093/gbe/evaa161

16. Gemmell, N., Haase, B., Formenti, G., Sims, Y., Wood, J., Howe, K., Mountcastle, J., Lillie, M., Olsson, M., Rhie, A., Fedrigo, O., and Jarvis, E. D. (2019). Lacerta agilis (Sand lizard) genome, rLacAgi1, primary haplotype. *Unpublished*. https://www.ncbi.nlm.nih.gov/assembly/GCF_009819535.1

17. Andrade, P., Pinho, C., Pérez i de Lanuza, G., Afonso, S., Brejcha, J., Rubin, C.-J., Wallerman, O., Pereira, P., Sabatino, S. J., Bellati, A., Pellitteri-Rosa, D., Bosakova, Z., Bunikis, I., Carretero, M. A., Feiner, N., Marsik, P., Paupério, F., Salvi, D., Soler, L., … Carneiro, M. (2019). Regulatory changes in pterin and carotenoid genes underlie balanced color polymorphisms in the wall lizard. *Proceedings of the National Academy of Sciences*, *116*, 5633–5642. https://doi.org/10.1073/pnas.1820320116

18. Roscito, J. G., Sameith, K., Pippel, M., Francoijs, K.-J., Winkler, S., Dahl, A., Papoutsoglou, G., Myers, G., and Hiller, M. (2018). The genome of the tegu lizard Salvator merianae : combining Illumina, PacBio, and optical mapping data to generate a highly contiguous assembly. *GigaScience*, *7*, 1–13. https://doi.org/10.1093/gigascience/giy141

19. Jezkova, T., Jaeger, J. R., Oláh-Hemmings, V., Jones, K. B., Lara-Resendiz, R. A., Mulcahy, D. G., and Riddle, B. R. (2016). Range and niche shifts in response to past climate change

in the desert horned lizard Phrynosoma platyrhinos. *Ecography*, *39*, 437–448. https://doi.org/10.1111/ecog.01464

20. Pasquesi, G. I. M., Adams, R. H., Card, D. C., Schield, D. R., Corbin, A. B., Perry, B. W., Reyes-Velasco, J., Ruggiero, R. P., Vandewege, M. W., Shortt, J. A., and Castoe, T. A. (2018). Squamate reptiles challenge paradigms of genomic repeat element evolution set by birds and mammals. *Nature Communications*, *9*, 2774. https://doi.org/10.1038/s41467-018-05279-1

21. Bronikowski, A., Fedrigo, O., Fungtammasan, C., Rhie, A., Mountcastle, J., Haase, B., Howe, K., Chow, W., Collins, J., and Jarvis, E. D. (2019). Thamnophis elegans (Western terrestrial garter snake) genome, rThaEle1, primary haplotype. *Unpublished*. https://www.ncbi.nlm.nih.gov/assembly/GCF_009769535.1

22. Suryamohan, K., Krishnankutty, S. P., Guillory, J., Jevit, M., Schröder, M. S., Wu, M., Kuriakose, B., Mathew, O. K., Perumal, R. C., Koludarov, I., Goldstein, L. D., Senger, K., Dixon, M. D., Velayutham, D., Vargas, D., Chaudhuri, S., Muraleedharan, M., Goel, R., Chen, Y.-J. J., … Seshagiri, S. (2020). The Indian cobra reference genome and transcriptome enables comprehensive identification of venom toxins. *Nature Genetics*, *52*, 106–117. https://doi.org/10.1038/s41588-019-0559-8

23. Hillier, L. W., Miller, W., Birney, E., Warren, W., Hardison, R. C., Ponting, C. P., Bork, P., Burt, D. W., Groenen, M. A. M., Delany, M. E., Dodgson, J. B., Chinwalla, A. T., Cliften, P. F., Clifton, S. W., Delehaunty, K. D., Fronick, C., Fulton, R. S., Graves, T. A., Kremitzki, C., … Wilson, R. K. (2004). Sequence and comparative analysis of the chicken genome provide unique perspectives on vertebrate evolution. *Nature*, *432*, 695–716. https://doi.org/10.1038/nature03154

24. Brian Simison, W., Parham, J. F., Papenfuss, T. J., Lam, A. W., and Henderson, J. B. (2020).

An Annotated Chromosome-Level Reference Genome of the Red-Eared Slider Turtle (Trachemys scripta elegans). *Genome Biology and Evolution*, *12*, 456–462. https://doi.org/10.1093/gbe/evaa063

25. Rhie, A., McCarthy, S. A., Fedrigo, O., Damas, J., Formenti, G., Koren, S., Uliano-Silva, M., Chow, W., Fungtammasan, A., Kim, J., Lee, C., Ko, B. J., Chaisson, M., Gedman, G. L., Cantin, L. J., Thibaud-Nissen, F., Haggerty, L., Bista, I., Smith, M., … Jarvis, E. D. (2021). Towards complete and error-free genome assemblies of all vertebrate species. *Nature*, *592*, 737–746. https://doi.org/10.1038/s41586-021-03451-0

26. Putnam, N. H., O'Connell, B. L., Stites, J. C., Rice, B. J., Blanchette, M., Calef, R., Troll, C. J., Fields, A., Hartley, P. D., Sugnet, C. W., Haussler, D., Rokhsar, D. S., and Green, R. E. (2016). Chromosome-scale shotgun assembly using an in vitro method for long-range linkage. *Genome Research*, *26*, 342–350. https://doi.org/10.1101/gr.193474.115

27. Pianka, E. R. (1991). Phrynosoma platyrhinos Girard Desert Horned Lizard. *Catalogue of American Amphibians and Reptiles*, *1981*, 1–4.

28. Leaché, Adam D., and Linkem, C. W. (2015). Phylogenomics of Horned Lizards (Genus: Phrynosoma) Using Targeted Sequence Capture Data. *Copeia*, *103*, 586–594. https://doi.org/10.1643/CH-15-248

29. Srikulnath, K., Nishida, C., Matsubara, K., Uno, Y., Thongpan, A., Suputtitada, S., Apisitwanich, S., and Matsuda, Y. (2009). Karyotypic evolution in squamate reptiles: comparative gene mapping revealed highly conserved linkage homology between the butterfly lizard (Leiolepis reevesii rubritaeniata, Agamidae, Lacertilia) and the Japanese four-striped rat snake (Elaphe quadrivirg. *Chromosome Research*, *17*, 975–986. https://doi.org/10.1007/s10577-009-9101-7

30. Rovatsos, M., Pokorná, M., Altmanová, M., and Kratochvíl, L. (2014). Cretaceous park of sex

determination: sex chromosomes are conserved across iguanas. *Biology Letters*, *10*, 20131093. https://doi.org/10.1098/rsbl.2013.1093

31. Grabherr, M. G. ., Brian J. Haas, Moran Yassour Joshua Z. Levin, Dawn A. Thompson, Ido Amit, Xian Adiconis, Lin Fan, Raktima Raychowdhury, Qiandong Zeng, Zehua Chen, Evan Mauceli, Nir Hacohen, Andreas Gnirke, Nicholas Rhind, Federica di Palma, Bruce W., N., and Friedman, and A. R. (2013). Trinity: reconstructing a full-length transcriptome without a genome from RNA-Seq data. *Nature Biotechnology*, *29*, 644–652. https://doi.org/10.1038/nbt.1883.Trinity

32. Cantarel, B. L., Korf, I., Robb, S. M. C., Parra, G., Ross, E., Moore, B., Holt, C., Sanchez Alvarado, A., and Yandell, M. (2007). MAKER: An easy-to-use annotation pipeline designed for emerging model organism genomes. *Genome Research*, *18*, 188–196. https://doi.org/10.1101/gr.6743907

33. Stanke, M., and Morgenstern, B. (2005). AUGUSTUS: a web server for gene prediction in eukaryotes that allows user-defined constraints. *Nucleic Acids Research*, *33*, W465–W467. https://doi.org/10.1093/nar/gki458

34. Blum, M., Chang, H.-Y., Chuguransky, S., Grego, T., Kandasaamy, S., Mitchell, A., Nuka, G., Paysan-Lafosse, T., Qureshi, M., Raj, S., Richardson, L., Salazar, G. A., Williams, L., Bork, P., Bridge, A., Gough, J., Haft, D. H., Letunic, I., Marchler-Bauer, A., … Finn, R. D. (2021). The InterPro protein families and domains database: 20 years on. *Nucleic Acids Research*, *49*, D344–D354. https://doi.org/10.1093/nar/gkaa977

35. Smit, AF, and Hubley, R. (2015). *RepeatModeler* (v. 1.0.11). http://www.repeatmasker.org

36. Smit, AFA, Hubley, R., and Green, P. (2015). *RepeatMasker* (v. 4.0.8). http://www.repeatmasker.org

37. Mi, H., Muruganujan, A., Casagrande, J. T., and Thomas, P. D. (2013). Large-scale gene function analysis with the PANTHER classification system. *Nature Protocols*, *8*, 1551–1566. https://doi.org/10.1038/nprot.2013.092

38. Mi, H., Ebert, D., Muruganujan, A., Mills, C., Albou, L.-P., Mushayamaha, T., and Thomas, P. D. (2021). PANTHER version 16: a revised family classification, tree-based classification tool, enhancer regions and extensive API. *Nucleic Acids Research*, *49*, D394–D403. https://doi.org/10.1093/nar/gkaa1106

39. da Silva, M. J., de Araújo Vieira, A. P., Galvão Cipriano, F. M., dos Santos Cândido, M. R., de Oliveira, E. H. C., Gimenez Pinheiro, T., and da Silva, E. L. (2020). The Karyotype of Salvator merianae (Squamata, Teiidae): Analyses by Classical and Molecular Cytogenetic Techniques. *Cytogenetic and Genome Research*, *160*, 94–99. https://doi.org/10.1159/000506140

40. Hill, M. O. (1973). Diversity and Evenness : A Unifying Notation and Its Consequences. *Ecology*, *54*, 427–432. https://www.jstor.org/stable/1934352

41. Leaché, A.D., and Sites, Jr., J. W. (2009). Chromosome Evolution and Diversification in North American Spiny Lizards (Genus *Sceloporus*). *Cytogenetic and Genome Research*, *127*, 166–181. https://doi.org/10.1159/000293285

42. Backstrom, N., Forstmeier, W., Schielzeth, H., Mellenius, H., Nam, K., Bolund, E., Webster, M. T., Ost, T., Schneider, M., Kempenaers, B., and Ellegren, H. (2010). The recombination landscape of the zebra finch Taeniopygia guttata genome. *Genome Research*, *20*, 485–495. https://doi.org/10.1101/gr.101410.109

43. Huttener, R., Thorrez, L., in't Veld, T., Granvik, M., Snoeck, L., Van Lommel, L., and Schuit, F. (2019). GC content of vertebrate exome landscapes reveal areas of accelerated protein evolution. *BMC Evolutionary Biology*, *19*, 144. https://doi.org/10.1186/s12862-019-1469-1

44. Schield, D. R., Card, D. C., Hales, N. R., Perry, B. W., Pasquesi, G. M., Blackmon, H., Adams, R. H., Corbin, A. B., Smith, C. F., Ramesh, B., Demuth, J. P., Betrán, E., Tollis, M., Meik, J. M., Mackessy, S. P., and Castoe, T. A. (2019). The origins and evolution of chromosomes, dosage compensation, and mechanisms underlying venom regulation in snakes. *Genome Research*, *29*, 590–601. https://doi.org/10.1101/gr.240952.118

45. Damas, J., Kim, J., Farré, M., Griffin, D. K., and Larkin, D. M. (2018). Reconstruction of avian ancestral karyotypes reveals differences in the evolutionary history of macro- and microchromosomes. *Genome Biology*, *19*, 155. https://doi.org/10.1186/s13059-018-1544-8

46. Axelsson, E., Webster, M. T., Smith, N. G. C., Burt, D. W., and Ellegren, H. (2005). Comparison of the chicken and turkey genomes reveals a higher rate of nucleotide divergence on microchromosomes than macrochromosomes. *Genome Research*, *15*, 120–125. https://doi.org/10.1101/gr.3021305

47. Smith, J., Bruley, C. K., Paton, I. R., Dunn, I., Jones, C. T., Windsor, D., Morrice, D. R., Law, A. S., Masabanda, J., Sazanov, A., Waddington, D., Fries, R., and Burt, D. W. (2000). Differences in gene density on chicken macrochromosomes and microchromosomes. *Animal Genetics*, *31*, 96–103. https://doi.org/10.1046/j.1365-2052.2000.00565.x

48. Kuraku, S., Ishijima, J., Nishida-Umehara, C., Agata, K., Kuratani, S., and Matsuda, Y. (2006). cDNA-based gene mapping and GC3 profiling in the soft-shelled turtle suggest a chromosomal size-dependent GC bias shared by sauropsids. *Chromosome Research*, *14*, 187–202. https://doi.org/10.1007/s10577-006-1035-8

49. Bolger, A. M., Lohse, M., and Usadel, B. (2014). Trimmomatic: a flexible trimmer for Illumina sequence data. *Bioinformatics*, *30*, 2114–2120. https://doi.org/10.1093/bioinformatics/btu170

50. Chapman, J. A., Ho, I., Sunkara, S., Luo, S., Schroth, G. P., and Rokhsar, D. S. (2011).

694 Meraculous: De Novo Genome Assembly with Short Paired-End Reads. *PLoS ONE*, *6*,
695 e23501. https://doi.org/10.1371/journal.pone.0023501

696 51. Lieberman-Aiden, E., van Berkum, N. L., Williams, L., Imakaev, M., Ragoczy, T., Telling, A.,
697 Amit, I., Lajoie, B. R., Sabo, P. J., Dorschner, M. O., Sandstrom, R., Bernstein, B., Bender,
698 M. A., Groudine, M., Gnirke, A., Stamatoyannopoulos, J., Mirny, L. A., Lander, E. S., and
699 Dekker, J. (2009). Comprehensive Mapping of Long-Range Interactions Reveals Folding
700 Principles of the Human Genome. *Science*, *326*, 289–293.
701 https://doi.org/10.1126/science.1181369

702 52. DovetailGenomics. (2015). *HiRise*.
703 https://github.com/DovetailGenomics/HiRise_July2015_GR

704 53. Zaharia, M., Bolosky, W. J., Curtis, K., Fox, A., Patterson, D., Shenker, S., Stoica, I., Karp, R.
705 M., and Sittler, T. (2011). *Faster and More Accurate Sequence Alignment with SNAP*. 1–10.
706 http://arxiv.org/abs/1111.5572

707 54. Leaché, Adam D., Banbury, B. L., Linkem, C. W., and de Oca, A. N.-M. (2016). Phylogenomics
708 of a rapid radiation: is chromosomal evolution linked to increased diversification in north
709 american spiny lizards (Genus Sceloporus)? *BMC Evolutionary Biology*, *16*, 63.
710 https://doi.org/10.1186/s12862-016-0628-x

711 55. Camacho, C., Coulouris, G., Avagyan, V., Ma, N., Papadopoulos, J., Bealer, K., and Madden,
712 T. L. (2009). BLAST+: architecture and applications. *BMC Bioinformatics*, *10*, 421.
713 https://doi.org/10.1186/1471-2105-10-421

714 56. Rice, E. S., Kohno, S., John, J. St., Pham, S., Howard, J., Lareau, L. F., O'Connell, B. L.,
715 Hickey, G., Armstrong, J., Deran, A., Fiddes, I., Platt, R. N., Gresham, C., McCarthy, F.,
716 Kern, C., Haan, D., Phan, T., Schmidt, C., Sanford, J. R., … Green, R. E. (2017). Improved
717 genome assembly of American alligator genome reveals conserved architecture of estrogen

718 signaling. *Genome Research*, *27*, 686–696. https://doi.org/10.1101/gr.213595.116

719 57. Bao, W., Kojima, K. K., and Kohany, O. (2015). Repbase Update, a database of repetitive
720 elements in eukaryotic genomes. *Mobile DNA*, *6*, 11. https://doi.org/10.1186/s13100-015-
721 0041-9

722 58. Simão, F. A., Waterhouse, R. M., Ioannidis, P., Kriventseva, E. V., and Zdobnov, E. M. (2015).
723 BUSCO: assessing genome assembly and annotation completeness with single-copy
724 orthologs. *Bioinformatics*, *31*, 3210–3212. https://doi.org/10.1093/bioinformatics/btv351

725 59. Georges, A., Li, Q., Lian, J., O'Meally, D., Deakin, J., Wang, Z., Zhang, P., Fujita, M., Patel,
726 H. R., Holleley, C. E., Zhou, Y., Zhang, X., Matsubara, K., Waters, P., Graves, J. A. M., Sarre,
727 S. D., and Zhang, G. (2015). High-coverage sequencing and annotated assembly of the
728 genome of the Australian dragon lizard Pogona vitticeps. *GigaScience*, *4*, 45.
729 https://doi.org/10.1186/s13742-015-0085-2

730 60. Liu, Y., Zhou, Q., Wang, Y., Luo, L., Yang, J., Yang, L., Liu, M., Li, Y., Qian, T., Zheng, Y., Li,
731 M., Li, J., Gu, Y., Han, Z., Xu, M., Wang, Y., Zhu, C., Yu, B., Yang, Y., … Gu, X. (2015).
732 Gekko japonicus genome reveals evolution of adhesive toe pads and tail regeneration.
733 *Nature Communications*, *6*, 10033. https://doi.org/10.1038/ncomms10033

734 61. Castoe, T. A., de Koning, A. J., Hall, K. T., Yokoyama, K. D., Gu, W., Smith, E. N., Feschotte,
735 C., Uetz, P., Ray, D. A., Dobry, J., Bogden, R., Mackessy, S. P., Bronikowski, A. M., Warren,
736 W. C., Secor, S. M., and Pollock, D. D. (2011). Sequencing the genome of the Burmese
737 python (Python molurus bivittatus) as a model for studying extreme adaptations in snakes.
738 *Genome Biology*, *12*, 406. https://doi.org/10.1186/gb-2011-12-7-406

739 62. Edwards J, R. (2018). Direct Submission. *Unpublished*.
740 https://www.ncbi.nlm.nih.gov/assembly/GCF_900518735.1

741 63. Aird, S. D., Arora, J., Barua, A., Qiu, L., Terada, K., and Mikheyev, A. S. (2017). Population
742 Genomic Analysis of a Pitviper Reveals Microevolutionary Forces Underlying Venom
743 Chemistry. *Genome Biology and Evolution*, *9*, 2640–2649.
744 https://doi.org/10.1093/gbe/evx199

745 64. Warren, W. C., and Wilson, R. K. (2015). Direct Submission. *Unpublished*.
746 https://www.ncbi.nlm.nih.gov/assembly/GCF_001077635.1/

747 65. St John, J. A., Braun, E. L., Isberg, S. R., Miles, L. G., Chong, A. Y., Gongora, J., Dalzell, P.,
748 Moran, C., Bed'Hom, B., Abzhanov, A., Burgess, S. C., Cooksey, A. M., Castoe, T. A.,
749 Crawford, N. G., Densmore, L. D., Drew, J. C., Edwards, S. V., Faircloth, B. C., Fujita, M. K.,
750 … Ray, D. A. (2012). Sequencing three crocodilian genomes to illuminate the evolution of
751 archosaurs and amniotes. *Genome Biology*, *13*, 415. https://doi.org/10.1186/gb-2012-13-1-
752 415

753 66. Wan, Q.-H., Pan, S.-K., Hu, L., Zhu, Y., Xu, P.-W., Xia, J.-Q., Chen, H., He, G.-Y., He, J., Ni,
754 X.-W., Hou, H.-L., Liao, S.-G., Yang, H.-Q., Chen, Y., Gao, S.-K., Ge, Y.-F., Cao, C.-C., Li,
755 P.-F., Fang, L.-M., … Fang, S.-G. (2013). Genome analysis and signature discovery for
756 diving and sensory properties of the endangered Chinese alligator. *Cell Research*, *23*, 1091–
757 1105. https://doi.org/10.1038/cr.2013.104

758 67. Wan, Q., Pan, S., Hu, L., Zhu, Y., Xu, P., Xia, J., Chen, H., He, G., He, J., Ni, X., Hou, H.,
759 Liao, S., Yang, H., Chen, Y., Gao, S., Ge, Y., Cao, C., Li, P., Fang, L., … Fang, S. (2014).
760 *Genomic data of the Chinese alligator (Alligator sinensis). GigaScience Database*.
761 http://dx.doi.org/10.5524/100077

762 68. Ghosh, A., Johnson, M. G., Osmanski, A. B., Louha, S., Bayona-Vásquez, N. J., Glenn, T. C.,
763 Gongora, J., Green, R. E., Isberg, S., Stevens, R. D., and Ray, D. A. (2020). A High-Quality
764 Reference Genome Assembly of the Saltwater Crocodile, Crocodylus porosus, Reveals

765 Patterns of Selection in Crocodylidae. *Genome Biology and Evolution*, *12*, 3635–3646.
766 https://doi.org/10.1093/gbe/evz269

767 69. Badenhorst, D., Hillier, L. W., Literman, R., Montiel, E. E., Radhakrishnan, S., Shen, Y., Minx,
768 P., Janes, D. E., Warren, W. C., Edwards, S. V., and Valenzuela, N. (2015). Physical
769 Mapping and Refinement of the Painted Turtle Genome (Chrysemys picta) Inform Amniote
770 Genome Evolution and Challenge Turtle-Bird Chromosomal Conservation. *Genome Biology*
771 *and Evolution*, *7*, 2038–2050. https://doi.org/10.1093/gbe/evv119

772 70. Deem, S. L., and Warren, W. C. (2018). Direct Submission. *Unpublished*.
773 https://www.ncbi.nlm.nih.gov/assembly/GCF_002925995.2

774 71. Wang, Z., Pascual-anaya, J., Zadissa, A., Li, W., and Niimura, Y. (2014). *Europe PMC*
775 *Funders Group The draft genomes of soft – shell turtle and green sea turtle yield insights*
776 *into the development and evolution of the turtle – specific body plan*. *45*, 701–706.
777 https://doi.org/10.1038/ng.2615.The

778 72. Venter, J. C., Adams, M. D., Myers, E. W., Li, P. W., Mural, R. J., Sutton, G. G., Smith, H. O.,
779 Yandell, M., Evans, C. A., Holt, R. A., Gocayne, J. D., Amanatides, P., Ballew, R. M., Huson,
780 D. H., Wortman, J. R., Zhang, Q., Kodira, C. D., Zheng, X. H., Chen, L., … Zhu, X. (2001).
781 The Sequence of the Human Genome. *Science*, *291*, 1304–1351.
782 https://doi.org/10.1126/science.1058040

783 73. Brent, M. R., Birren, B. W., Antonarakis, S. E., Alexandersson, M., Zody, M., Birney, E.,
784 Baertsch, R., Cuff, J., Parra, G., Slater, G., Waterston, R. H., Lindblad-Toh, K., Rogers, J.,
785 Abril, J. F., Agarwal, P., Agarwala, R., Ainscough, R., An, P., Attwood, J., … Lander, E. S.
786 (2002). Initial sequencing and comparative analysis of the mouse genome. *Nature*, *420*,
787 520–562. https://doi.org/10.1038/nature01262

788 74. Bateman, A. (2019). UniProt: a worldwide hub of protein knowledge. *Nucleic Acids Research*,

47, D506–D515. https://doi.org/10.1093/nar/gky1049

75. Card, D. C. (2020). *Orthorbb* (v. 2.2). https://github.com/darencard/GenomeAnnotation/blob/master/orthorbb

76. Jones, P., Binns, D., Chang, H.-Y., Fraser, M., Li, W., McAnulla, C., McWilliam, H., Maslen, J., Mitchell, A., Nuka, G., Pesseat, S., Quinn, A. F., Sangrador-Vegas, A., Scheremetjew, M., Yong, S.-Y., Lopez, R., and Hunter, S. (2014). InterProScan 5: genome-scale protein function classification. *Bioinformatics*, *30*, 1236–1240. https://doi.org/10.1093/bioinformatics/btu031

77. Schield, D. R. (2017). *Slidingwindow_gc_content.py*. https://github.com/drewschield/Comparative-Genomics-Tools

78. McKenna, D. D., Scully, E. D., Pauchet, Y., Hoover, K., Kirsch, R., Geib, S. M., Mitchell, R. F., Waterhouse, R. M., Ahn, S.-J., Arsala, D., Benoit, J. B., Blackmon, H., Bledsoe, T., Bowsher, J. H., Busch, A., Calla, B., Chao, H., Childers, A. K., Childers, C., … Richards, S. (2016). Genome of the Asian longhorned beetle (Anoplophora glabripennis), a globally significant invasive species, reveals key functional and evolutionary innovations at the beetle–plant interface. *Genome Biology*, *17*, 227. https://doi.org/10.1186/s13059-016-1088-8

79. Koochekian, N., Ascanio, A., Farleigh, K., Card, D. C., Schield, D. R., Castoe, T. A., and Jezkova, T. (2021). Supporting data for “A chromosome-level genome assembly and annotation of the desert horned lizard, Phrynosoma platyrhinos, provides insight into chromosomal rearrangements among reptiles.” *GigaScience Database*. http://dx.doi.org/10.5524/100948

80. Hedges, S. B., Dudley, J., and Kumar, S. (2006). TimeTree: a public knowledge-base of divergence times among organisms. *Bioinformatics*, *22*, 2971–2972.

https://doi.org/10.1093/bioinformatics/btl505

FIGURES

Figure 1. For each major clade, we list diploid chromosome numbers, macrochromosome numbers, and microchromosome numbers based on previous research [1]. The phylogeny was adapted from [2].

Figure 2. The genome content of P. platyrhinos. The outer circle shows gene density on each chromosome, the middle circle shows repeat element density, and the inner one shows GC content. Each estimate is calculated per 1 million base pair window in each chromosome. “Ma” indicates macrochromosomes and “mi” stands for microchromosomes. Two scaffolds for macrochromosome 3 are attached together (the black line) and two microchromosomes (mi6 and mi10) resulted from a single scaffold were showed separately and in size order with the rest of the microchromosomes.

Figure 3. Synteny between *P. platyrhinos* and 12 reptilian taxa: three snakes (*N. naja*, *T. elegance*, and *C. viridis*), five lizards *(A. carolinensis, L. agilis, Z. vivipara, P. muralis*, and *S. merianae*), three turtles (*T. scripta, G. evgoodei*, and *D. coriacea*), and a bird (*G. gallus*). The cladogram shows the phylogenetic relationships among the sampled taxa [80] (two scaffolds for macrochromosome 3 (3a and 3b) are concatenated in this figure).

Figure 4. Effective number of chromosomes (C) assessed using the dominance analysis. Values close to 1 represent full dominance (homologies from a given *P. platyrhinos* chromosome are contained within a single chromosome/scaffold of another species). Values higher than 1 mean a spread of homologies across multiple chromosomes/scaffolds.

Figure 5. Summary of the effective number of chromosomes of P. platyrhinos in comparison with the 12 target species based on SR a) Mean and SD of SR for each chromosome among 12 species. Values close to 1 represent full dominance (homologies from a given P. platyrhinos chromosome are contained within a single chromosome/scaffold). Values higher than 1 mean a spread of homologies across multiple chromosomes/scaffolds. b) Cumulative SR for chromosomes of 12 reptilian species. The total amount of SR at greater phylogenetic distances,

841 is higher (cumulative SR ~ 30 in turtles) and showing greater rearrangements and partitions of syntenic blocks in
842 macrochromosomes than in microchromosomes

843

844 Figure 6. Synteny between *P. platyrhinos* potential microchromosomes (before assigning scaffolds to specific
845 chromosomes) and the 12 reptilian genomes. The cladogram shows the phylogenetic relationships among the
846 assessed taxa [80].

847

848 Figure S1: Repeat elements, GC content, and gene density calculated in 1Mb windows for each chromosome of *P.*
849 *platyrhinos* (two scaffolds for macrochromosome 3 are concatenated).

850

851 Figure S2: Proportion of identified gene IDs from protein-coding annotation to unidentified gene IDs by PANTHER a)
852 across the chromosomes (Ma stands for macrochromosome, and mi stands for microchromosome). b) between two
853 groups of chromosomes (Macros = macrochromosomes, and Micros = microchromosomes).

854

855 Figure S2. Investigating potential misassembled point on a final scaffold. a) Chicago scaffolds assembled to a final
856 scaffold “Sc4326_4427” were used to investigate a possible misassembled point. b) repeat elements, GC content,
857 and gene density calculated in 1Mb windows were used as evidence to find break point on this final scaffold. Outlined
858 cells are where the breakpoint was placed. Then microchromosomes were numbered based on size so these two
859 scaffolds were numbered as microchromosome 10 (left portion) and microchromosome 6 (right portion).

860

861 Figure S4: Distribution of *P. platyrhinos* total annotated protein coding genes with identified IDs in PANTHER database.
862 Among 164 PANTHER pathways assigned to *P. platyrhinos* protein coding genes, each pathway accounts for different
863 number of genes (2< genes per pathway <759) that may belong to a specific chromosome (24 pathways only on
864 macrochromosomes, and 3 only on microchromosomes) or group of chromosomes (13 pathways only in
865 macrochromosomes group).

866

TABLES

Table 1. Basic information about the *P. platyrhinos* genome assembly.

Assembly	Chicago Assembly	Chicago + Hi-C Assembly
Longest Scaffold (bp)	361,415,485	396,190.715
Number of Scaffolds	5,458	5,294
Number of Scaffolds > 1 kb	5,458	5,294
Contig N50 (kb)	12.04	12.04
Scaffold N50 (kb)	63,431	273,213
Number of Gaps	258,150	258,317
Percent of Genome in Gaps	1.54%	1.54%

Table 2: BUSCO summary results.

BUSCO benchmark	Number		Percentage	
Present BUSCOs	4,324		81.5%	
Complete BUSCOs	3640		68.6%	
Complete single-copy BUSCOs		3609		68.0%
Complete duplicated BUSCOs		31		0.6%
Fragmented BUSCOs	684		12.9%	
Missing BUSCOs	986		18.5%	
Total BUSCO groups searched	5310		100	

873 Table 3**.** Sequencing libraries used for the genome assembly of *P. platyrhinos.*

Library	Read Type	Number of Reads	Assembly Version	NCBI accession number
Shotgun library 1 (150 bp)	paired end	311,540,000	Primary	SRR16071941
Shotgun library 2 (150 bp)	paired end	239,630,000	Primary	SRR16071940
Shotgun library 3 (150 bp)	paired end	308,750,000	Primary	SRR16071939
Chicago library 1 (151 bp)	paired end	402,000,000	Intermediate	SRR13811242
Chicago library 2 (151 bp)	paired end	398,000,000	Intermediate	SRR13811241
Chicago library 3 (151 bp)	paired end	256,000,000	Intermediate	SRR13811240
Hi-C library 1 (151 bp)	paired end	332,000,000	Final	SRR13811239
Hi-C library 2 (151 bp)	paired end	374,000,000	Final	SRR13811238
Hi-C library 3 (151 bp)	paired end	324,000,000	Final	SRR13811237

874

875 Table 4. Number of reads obtained from 8 tissues of *P. platyrhinos*, used for transcriptome assembly.

Sample ID	Tissue	Raw Reads	Quality Trimmed Reads	NCBI accession number
TRO180600001	liver	49,736,350	47,699,266	SRR13326553
TRO180600002	lungs	40,643,066	39,124,052	SRR13326552
TRO180600003	brain	85,097,044	81,754,486	SRR13326551
TRO180600004	muscle	37,712,026	34,653,428	SRR13326550
TRO180600005	testes	62,536,762	58,283,654	SRR13326549
TRO180600006	heart	34,757,154	32,027,338	SRR13326548
TRO180600007	eyes	46,140,488	42,334,272	SRR13326547
TRO180600008	kidneys	41,776,926	38,635,176	SRR13326546

876

Table S1. The corresponding scaffolds (first column) for each chromosome of *P. platyrhinos* (second column) and scaffold length (third column) in base pairs. *This scaffold was broken down into two microchromosomes (6 and 10).

Scaffold name	Chromosome(s) name	length (in base pairs)
Sc3291_377	Chromosome 1	396,190,715
Sc439 _455	Chromosome 2	336,734,411
Sc1234_1274	Chromosome 3-a	178,616,284
Sc1882_1940	Chromosome 3-b	123,146,639
Sc5292_5410	Chromosome 4	273,212,746
Sc5293_5450	Chromosome 5	219,432,639
Sc521_540	Chromosome 6	129,273,435
Sc3285_3371	Microchromosome 1	31,685,405
Sc3778_3872	Microchromosome 2	28,086,253
Sc415_430	Microchromosome 3	27,277,973
Sc35_37	Microchromosome 4	27,087,043
Sc3441_3531	Microchromosome 5	26,097,904
Sc4326_4427*		
Sc4326a4427	Microchromosome 10	11,894,615
Sc4326b4427	microchromosome 6	23,702,528
Sc26_27	Microchromosome 7	20,466,995
Sc5294_5452	Microchromosome 8	16,009,790
Sc1213_1253	Microchromosome 9/X	15,721,303
Sc953_986	Microchromosome 11	8,897,685

880 Table S2. Best blast hits of cDNA [29] and * indicates sex linked markers [30] from *A. carolinensis* and *L.*

881 *reevesii* against the genome of *P. platyrhinos*.

Marker	Accession	Chromosomal location			E-value
		A. carolinensis	*L. reevesii*	*P. platyrhinos*	
DYNC1H1	AB490348		1q	Chr1	2.95E-179
ESR1	AB490345		1p	Chr1	1.02E-113
WT1	XM_016992885	1		Chr1	2.19E-158
WT1	AB490347		1q	Chr1	7.53E-80
XAB1	AB490344		1p	Chr1	2.31E-35
CHD1	XM_008103079	2		Chr2	0
CHD1	AB480289		2p	Chr2	1.25E-144
DMRT1	XM_003216553	2		Chr2	0
DMRT1	AB480288		2p	Chr2	2.15E-64
GHR	XM_008102837	2		Chr2	0
GHR	AB480290		2p	Chr2	1.01E-104
RPS6	XM_003216606	2		Chr2	5.32E-123
RPS6	AB480287		2p	Chr2	2.39E-88
RUFY1	XM_008104854	2		Chr2	0
RUFY1	AB490352		2q	Chr2	3.45E-22
EIF2S3	XM_003218845	3		Chr3-a	0
EIF2S3	AB490361		3q	Chr3-a	5.58E-104
OCA2	XM_008107106	3		Chr3-a	0
OCA2	AB490360		3q	Chr3-a	1.78E-89
SH3PXD2A	XM_016992171	3		Chr3-b	0
SH3PXD2A	AB490356		3p	Chr3-b	5.98E-166
TLOC1	AB490355	3p		Chr3-b	1.71E-79
HDAC3	XM_003219886	4		Chr4	0
HDAC3	AB490365		4p	Chr4	4.16E-97
RBM12	XM_008109953	4		Chr4	0
RBM12	AB490367		4q	Chr4	3.92E-137

SS18	XM_003219645	4		Chr4	0
SS18	AB490397		4p	Chr4	1.75E-70
ZNF326	XM_008109275	4		Chr4	0
ZNF326	AB490366		4q	Chr4	1.00E-128
ACSL1	XM_008111814	5		Chr5	0
ACSL1	AB490370		5p	Chr5	1.00E-95
DCLK2	XM_008111991	5		Chr5	0
DCLK2	AB490369		5p	Chr5	2.06E-73
EXOC1	XM_008111693	5		Chr5	0
EXOC1	AB490371		5p	Chr5	3.08E-176
RANGAP1	XM_008110743	5		Chr5	0
RANGAP1	AB490374		5q	Chr5	6.70E-80
SOX5	XM_008110345	5		Chr5	0
SOX5	AB490376		5q	Chr5	1.78E-104
UCHL1	XM_003221541	5		Chr5	2.55E-63
UCHL1	AB490372		5p	Chr5	3.46E-59
CTNNB1	AB490379		6q	Chr6	0
GAD2	XM_003222133	6		Chr6	0
GAD2	AB490380		6q	Chr6	1.98E-76
MYST2	AB490378		6p	Chr6	0
WAC	XM_008112381	6		Chr6	0
WAC	AB490381		6q	Chr6	3.60E-159
AR	AB490385		micro	microchr3	2.72E-152
TMEM132D*	XM_008113640.2	micro “b”/X		microchr9/X	0
FZD10*	XM_003222753.3	micro “b”/X		microchr9/X	0
ATP2A2*	XM_008113715	micro “b”/X		microchr9/X	0
ATP2A2	AB490391		micro	microchr9/X	4.05E-167
ATRX	AB490386		micro	microchr3	7.88E-127
BRD7	AB490390		micro	microchr2	3.95E-68
HSPA8	XM_003222794	micro “a”		Chr1	0
HSPA8	AB490395		micro	microchr4	3.70E-162

882

883 Table S3. Number, length, and percentage of annotated repeat elements identified.

Families of repeat elements	Numbers of elements	Length masked (bp)	% of sequence	% element masked
Retroelements	2,082,017	451,287,018	23.83	20.37
SINEs	648,720	89,280,596	4.72	6.35
Penelope	254,722	35,799,757	1.89	2.50
LINEs	1,311,944	319,965,632	16.90	12.84
L2/CR1/Rex	702,907	160,952,766	8.50	6.88
R1/LOA/Jockey	36	3,068	0.00	0.00
R2/R4/NeSL	5,129	640,551	0.03	0.05
RTE/Bov-B	257,696	83,172,778	4.39	2.52
L1/CIN4	87,958	38,708,200	2.04	0.86
LTR elements	121,353	42,040,790	2.22	1.19
BEL/Pao	4,074	768,559	0.04	0.04
Ty1/Copia	18,376	7,918,963	0.42	0.18
Gypsy/DIRS1	39,227	14,661,509	0.77	0.38
Retroviral	34,521	5,663,234	0.30	0.34
DNA transposons	1,527,111	204,435,133	10.80	14.94
hobo-Activator	610,832	73,847,731	3.90	5.98
Tc1-IS630-Pogo	314,462	42,728,561	2.26	3.08
PiggyBac	1,795	445,424	0.02	0.02
Tourist/Harbinger	500,329	78,020,620	4.12	4.90
Unclassified	828,472	146,176,330	7.72	8.11
Total interspersed repeats	9,351,681	801,898,481	42.35	91.51
Small RNA	33,490	3,376,969	0.18	0.33
Satellites	51,860	7,242,936	0.38	0.51
Simple repeats	705,413	27,116,672	1.43	6.90
Low complexity	77,452	3,957,871	0.21	0.76

Total masked	10,219,896	841,750,763	44.45	100.00

884

885 Table S4: Comparison of molecular pathways analysis on macrochromosomes and microchromosomes. Second
886 column shows the specific pathways identified on each chromosome. Third column shows the pathways that belong
887 to specific group of chromosomes.

Chromosome location	Specific pathways for each chromosome	Specific pathways for macros versus micros
Chromosome 1	Allantoin degradation (P02725), Methionine biosynthesis (P02753)	5-Hydroxytryptamine biosynthesis (P04371), Acetate utilization (P02722), Activin beta signaling pathway (P06210), Anandamide degradation (P05728), Androgen/estrogene/progesterone biosynthesis (P02727), Ascorbate degradation (P02729), ATP synthesis (P02721), Biotin biosynthesis (P02731), BMP/activin signaling pathway-drosophila (P06211), DPP signaling pathway (P06213), DPP-SCW signaling pathway (P06212), Glutamine glutamate conversion (P02745), Isoleucine biosynthesis (P02748), Leucine biosynthesis (P02749), Methylmalonyl pathway (P02755), Proline biosynthesis (P02768), Purine metabolism (P02769), Pyridoxal phosphate salvage pathway (P02770), Pyridoxal-5-phosphate biosynthesis (P02759), SCW signaling pathway (P06216), Succinate to proprionate conversion (P02777), Toll pathway-drosophila (P06217), Valine biosynthesis (P02785), and Vitamin B6 metabolism (P02787)
Chromosome 2	ALP23B signaling pathway (P06209), GBB signaling pathway (P06214), MYO signaling pathway (P06215)	
Chromosome 3	Cysteine biosynthesis (P02737), Lysine biosynthesis (P02751)	
Chromosome 4	Thiamin metabolism (P02780)	
Chromosome 5	Cobalamin biosynthesis (P02735), Sulfate assimilation (P02778)	
Chromosome 6	Carnitine metabolism (P02733), Coenzyme A linked carnitine metabolism (P02732), and Threonine biosynthesis (P02781)	
Microchromosome 1	None.	None.
Microchromosome 2	Tyrosine biosynthesis (P02784)	
Microchromosome 3	None.	

	Bupropion degradation
Microchromosome 4	(P05729)
	Triacylglycerol metabolism
Microchromosome 5	(P02782)
Microchromosome 6	None.
Microchromosome 7	None.
Microchromosome 8	None.
Microchromosome 9/X	None.
Microchromosome10	None
Microchromosome 11	None.

888

889

890

Table S5. Genome assemblies and number of markers used for *in silico* painting. All assemblies are available through NCBI under the appropriate accession.

Organism	Potential single markers	Total confirmed (5 consecutive) markers	Scaffolds with confirmed homologies	Confirmed markers in Scaffolds (%)	Assembly accession
A. carolinensis	2,616,045	87,155	13	57,006 (65.41)	GCA_000090745.2
S. merianae	390,847	31,955	19	31,805 (99.53)	GCA_003586115.2
L. agilis	755,639	44,200	20	44,199 (99.99)	GCA_009819535.1
P. muralis	719,822	46,093	19	45,731 (99.21)	GCA_004329235.1
Z. vivipara	751,121	43,371	19	42,224 (97.35)	GCA_011800845.1
C. viridis	299,173	18,161	18	17,891 (98.51)	GCA_003400415.2
T. elegans	282,458	17,817	18	17,725 (99.48)	GCA_009769535.1
N. naja	291, 209	19,898	19	19,805 (99.52)	GCA_009733165.1
T. scripta	177,241	15,287	25	15,252 (99.77)	GCA_013100865.1
G. evgoodei	152,748	14,864	24	14,614 (98.32)	GCA_007399415.1
D. coriacea	137,161	14,075	29	14,075 (100.00)	GCA_009764565.3
G. gallus	88,397	10,934	33	10,934 (100.00)	GCA_000002315.5

Figure1

Click here to access/download;Figure;fig1.docx

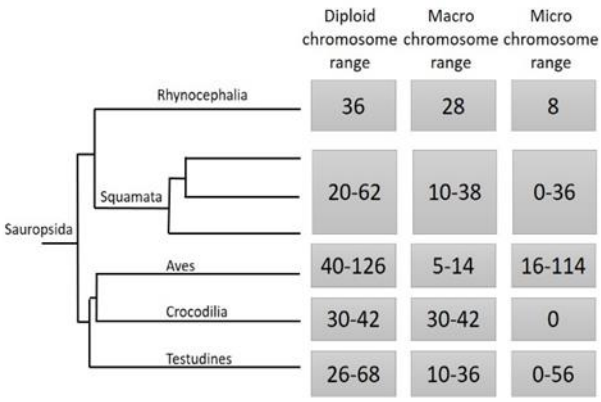

Figure2

Click here to access/download;Figure;Figure2.jpg

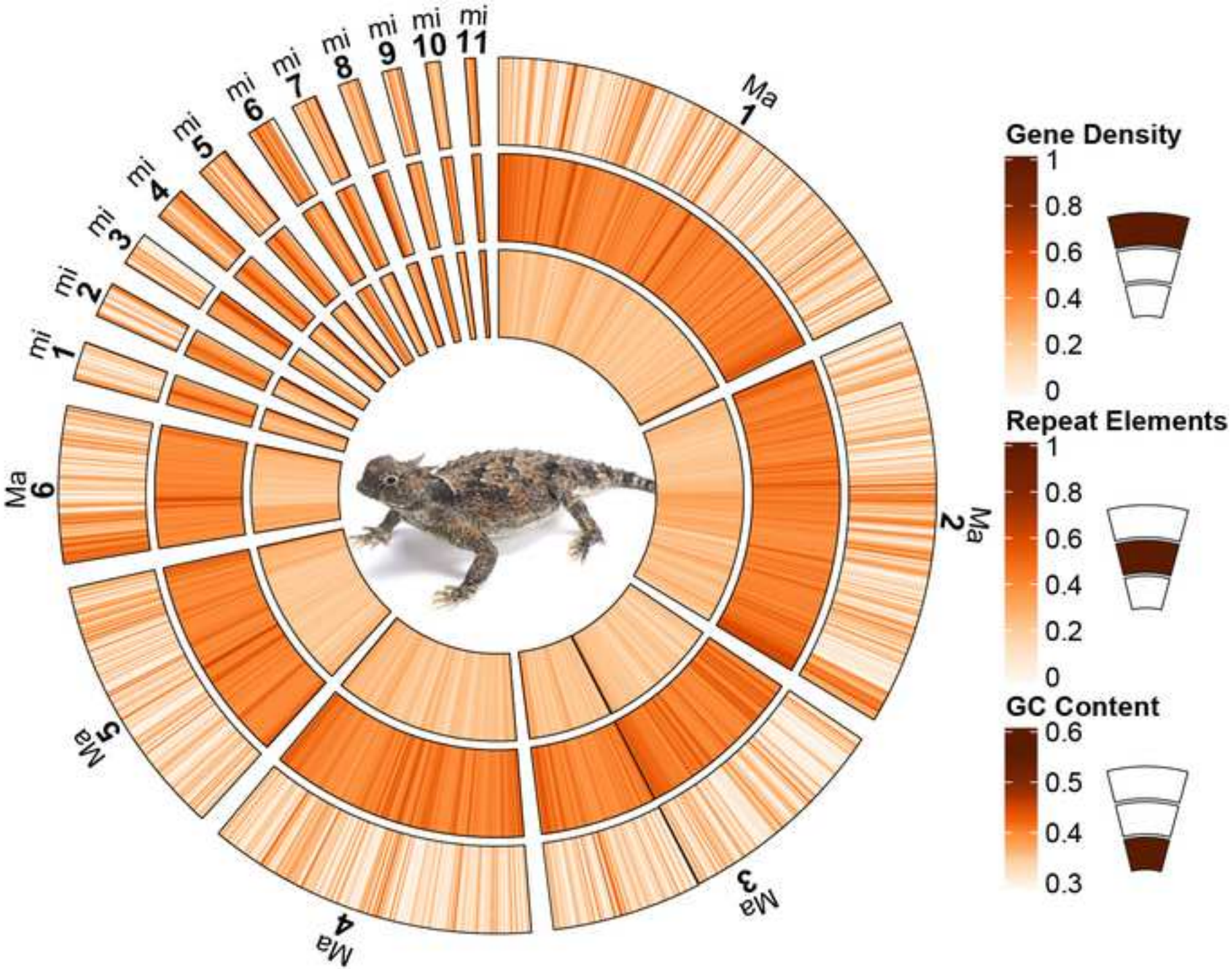

Figure3

Click here to access/download;Figure;Figure3.jpg

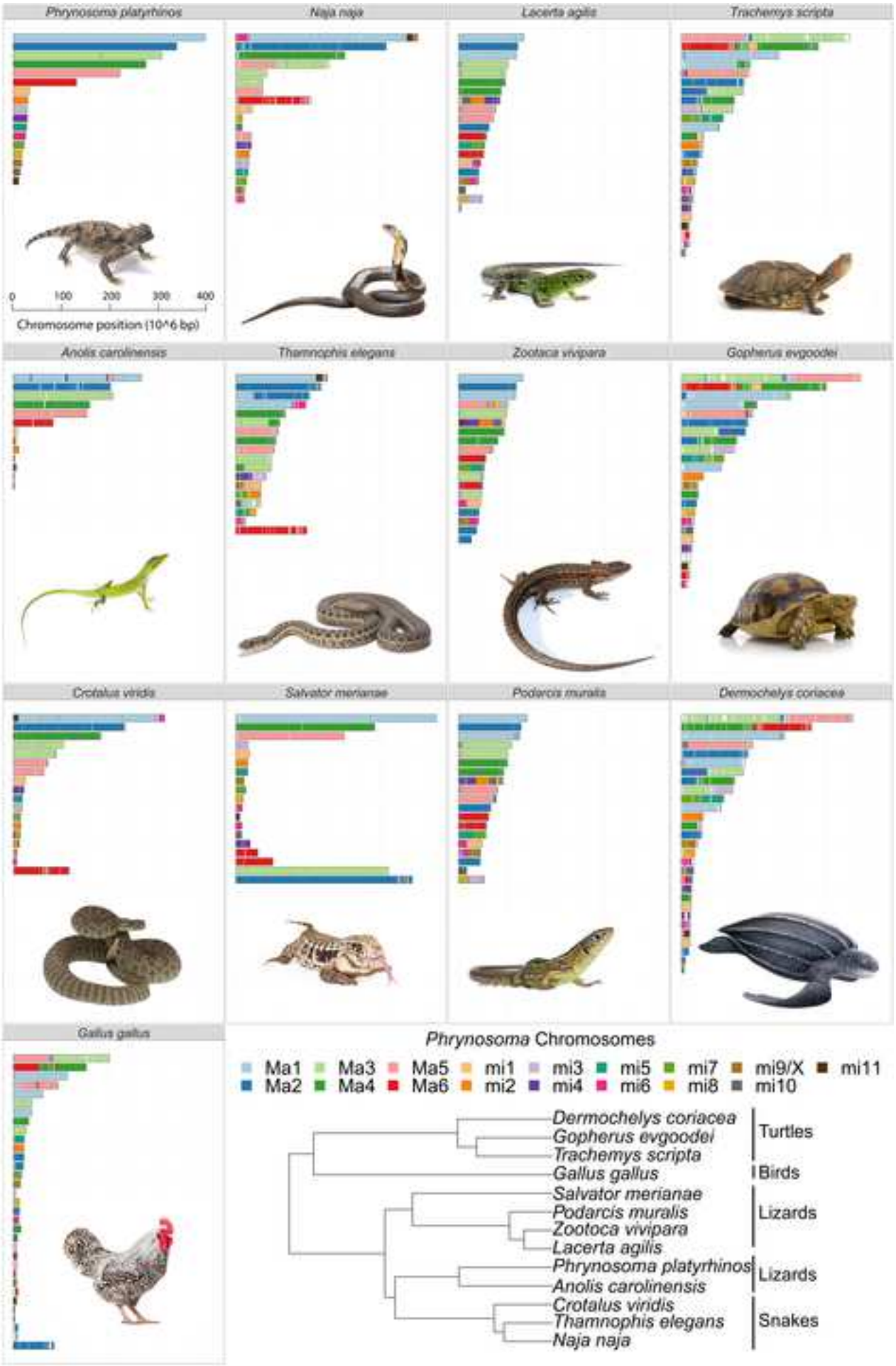

Figure4

Click here to access/download;Figure;fig4.docx

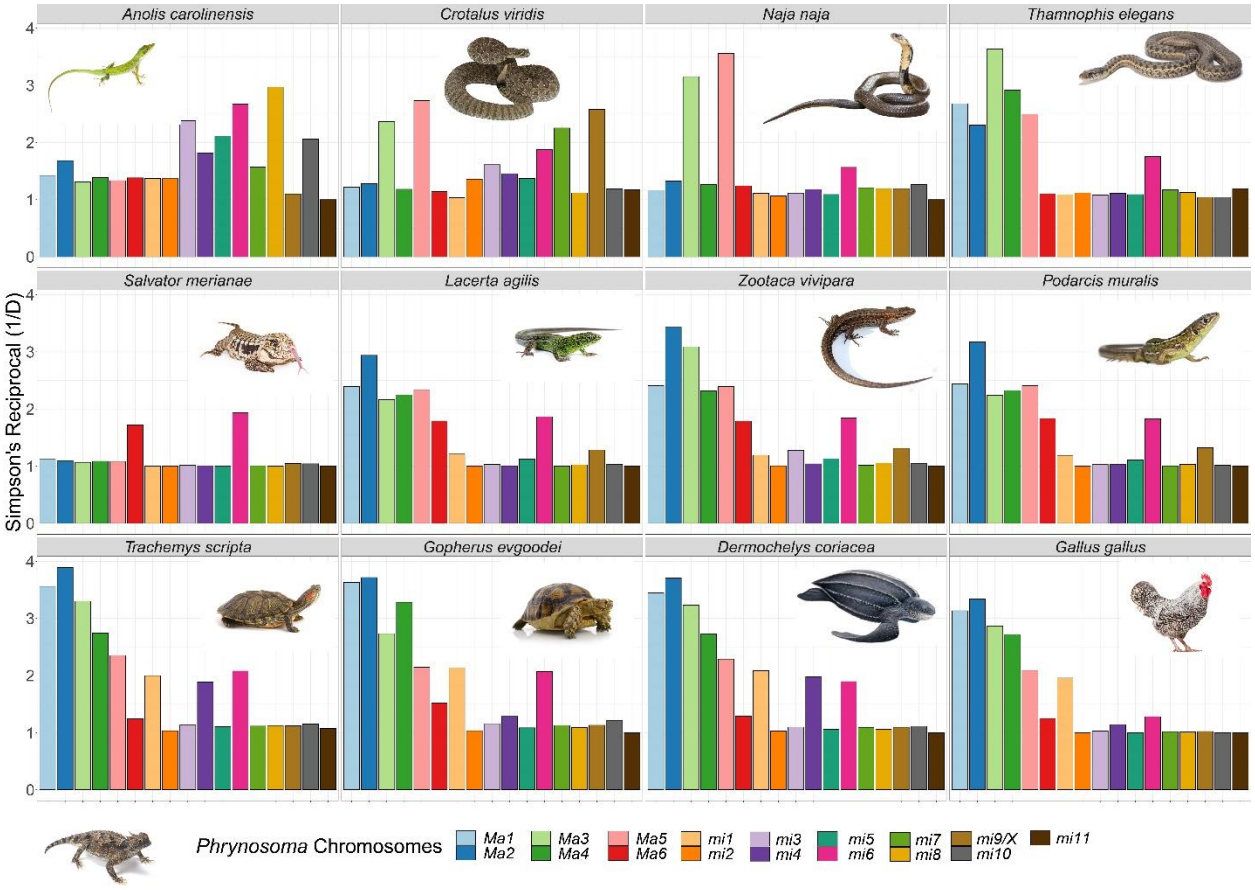

Figure5a

Click here to access/download;Figure;Figure5a.jpg

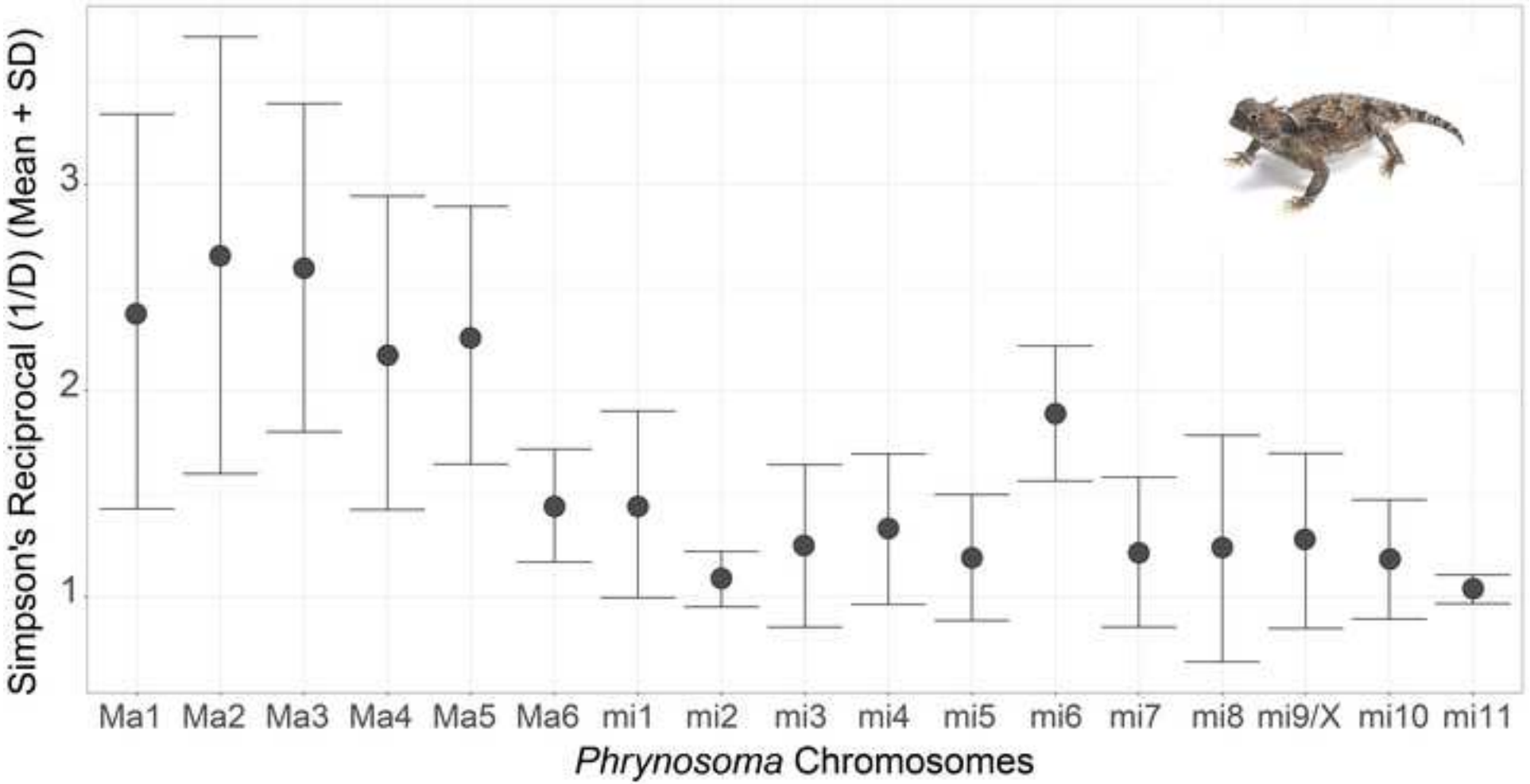

Figure5b

Click here to access/download;Figure;Figure5b.jpg

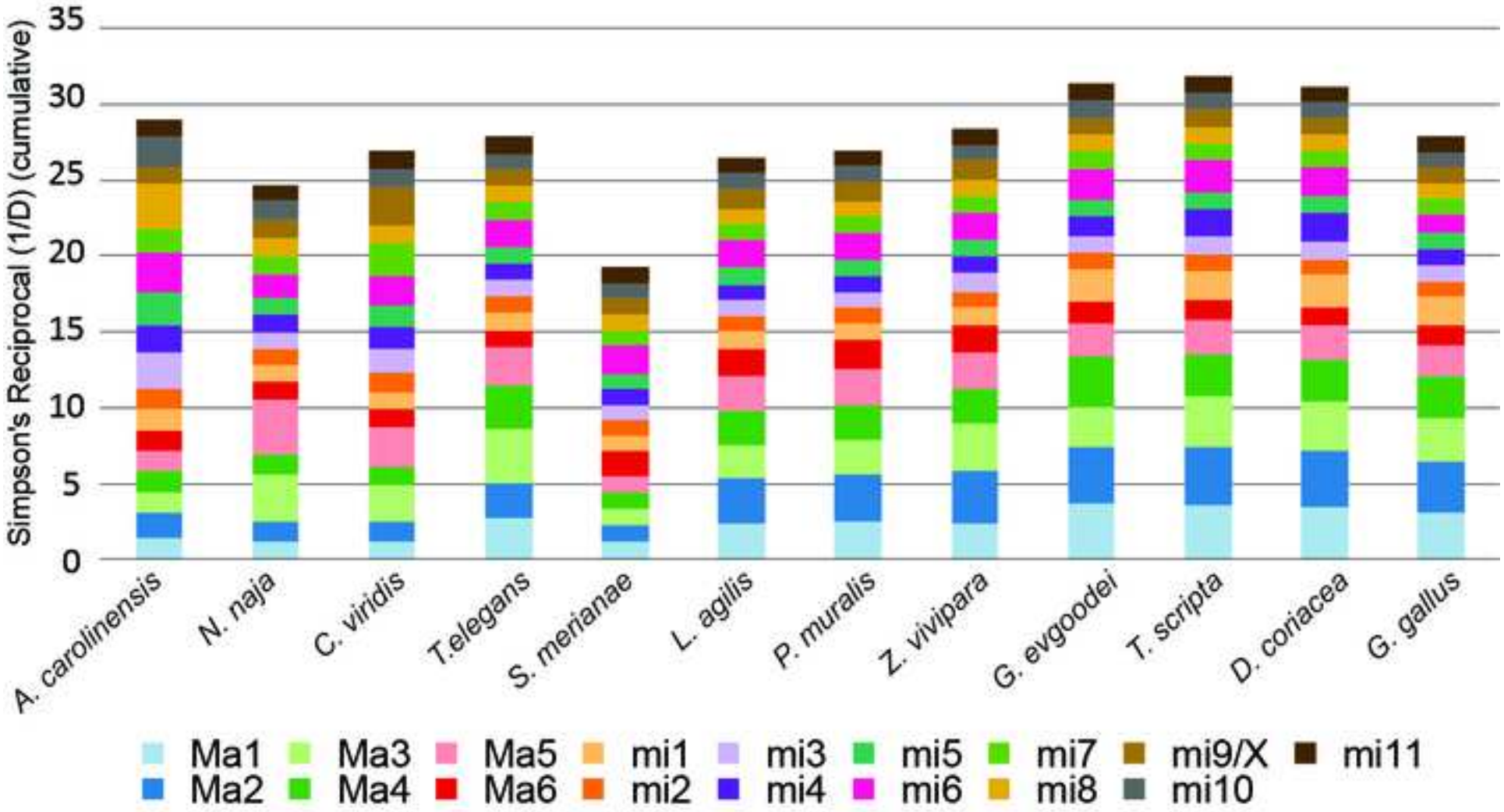

Figure6

Click here to access/download;Figure;Figure6.jpg

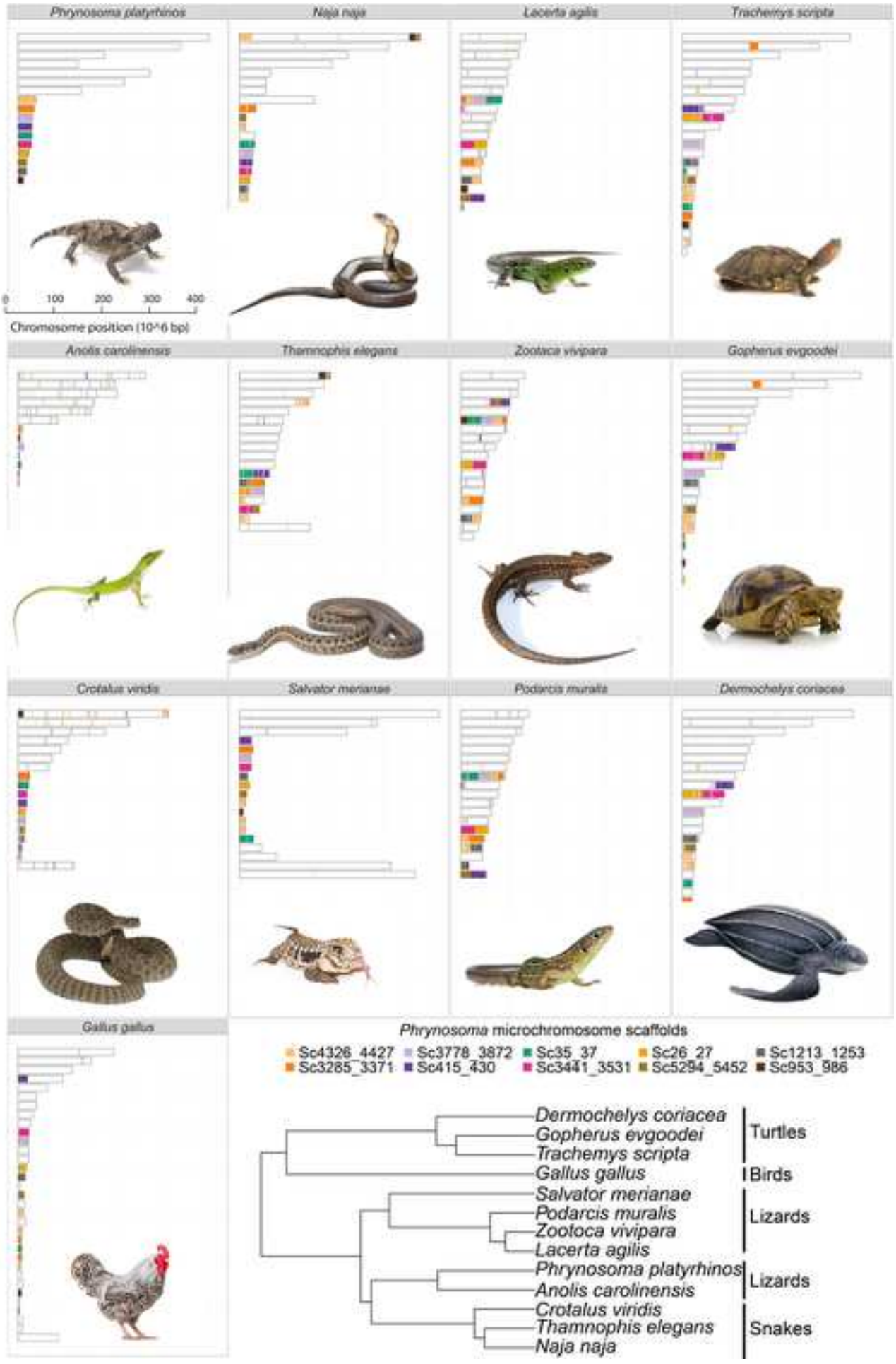

FigurS1

Click here to access/download;Figure;FigureS1.jpg

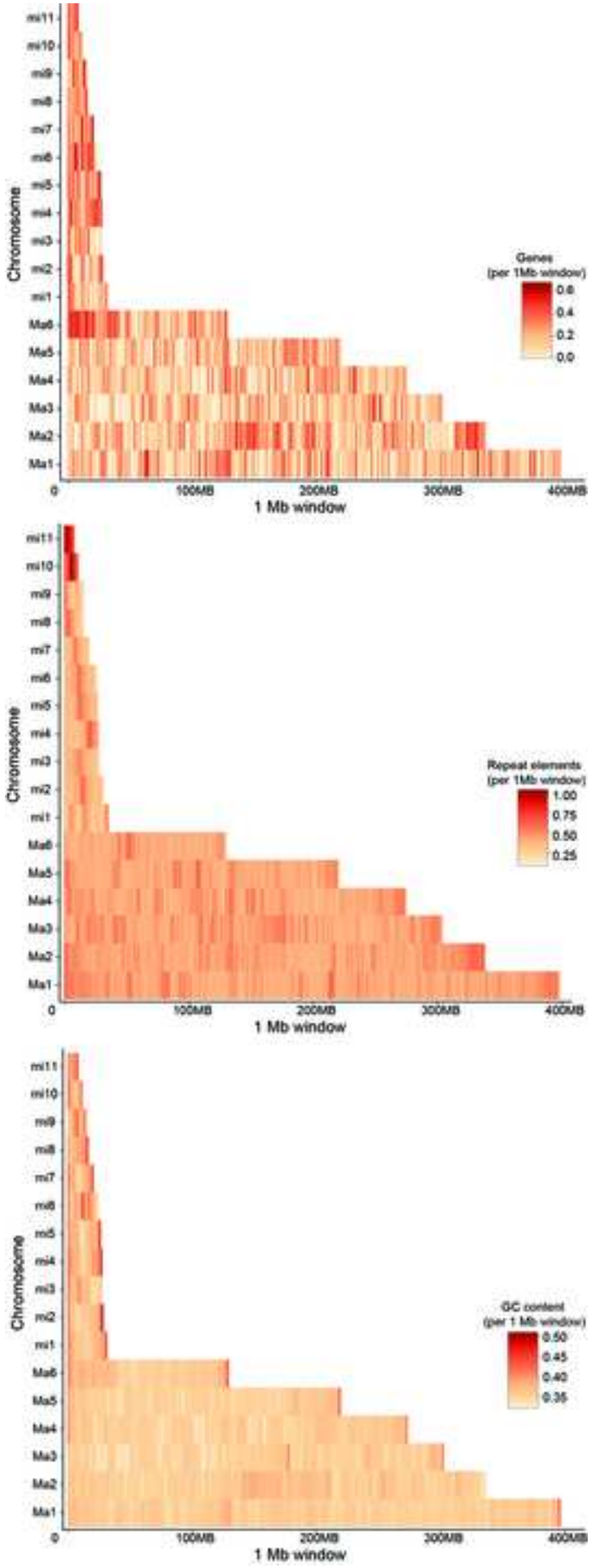

FigurS2a

Click here to access/download;Figure;FigureS2a.jpg

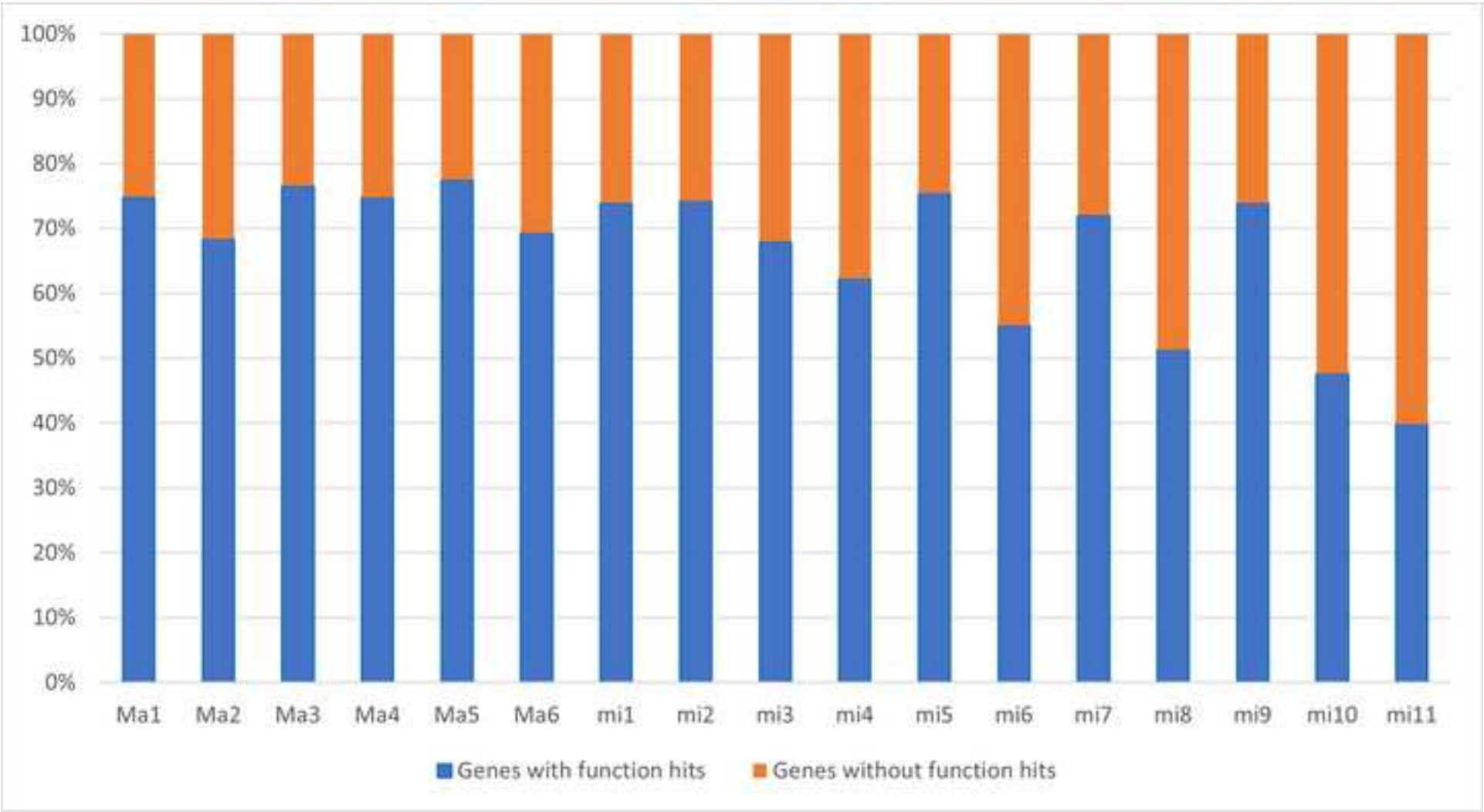

FigurS2b

Click here to access/download;Figure;FigureS2b.jpg

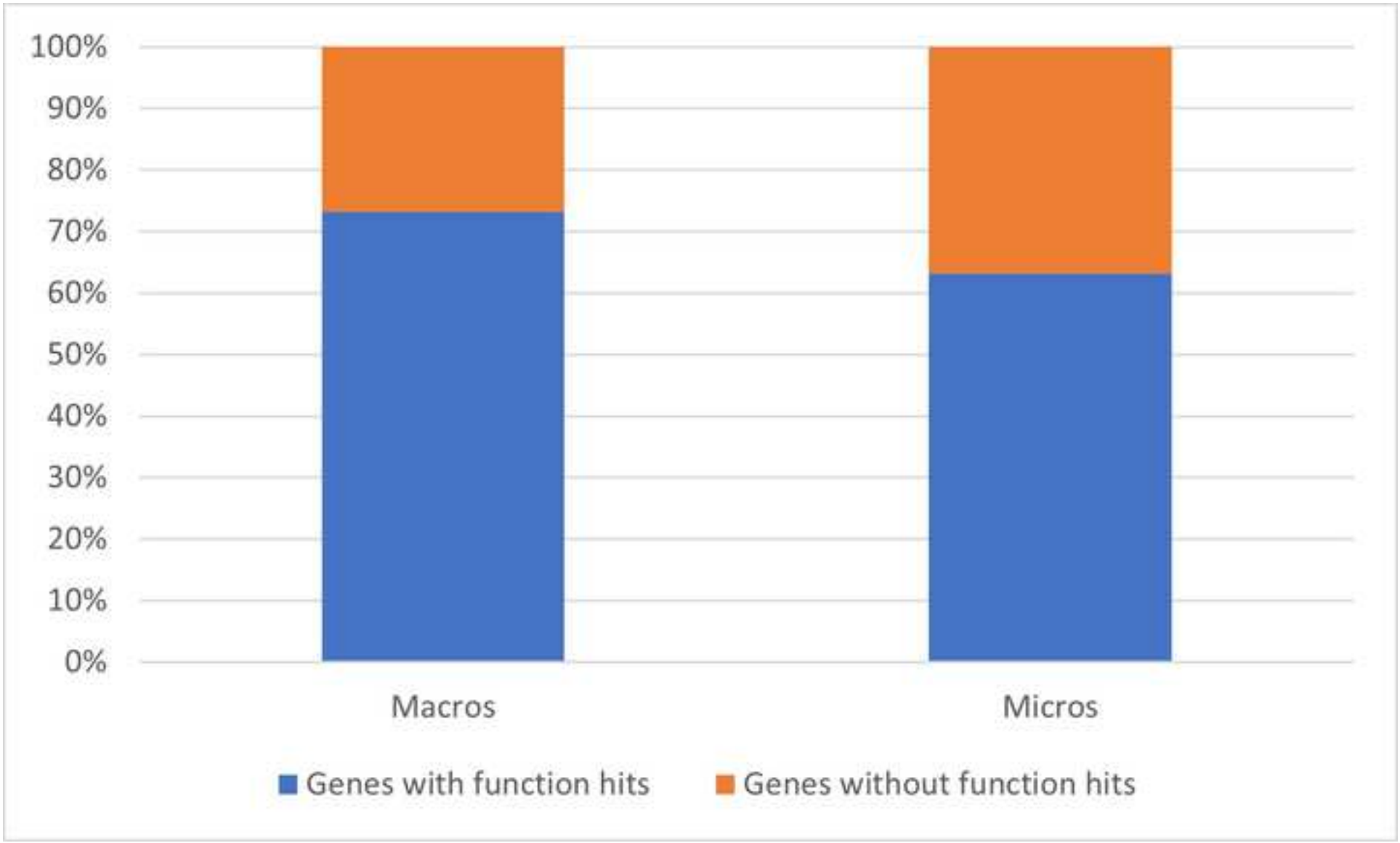

FigurS3

Click here to access/download;Figure;FigureS3.jpg

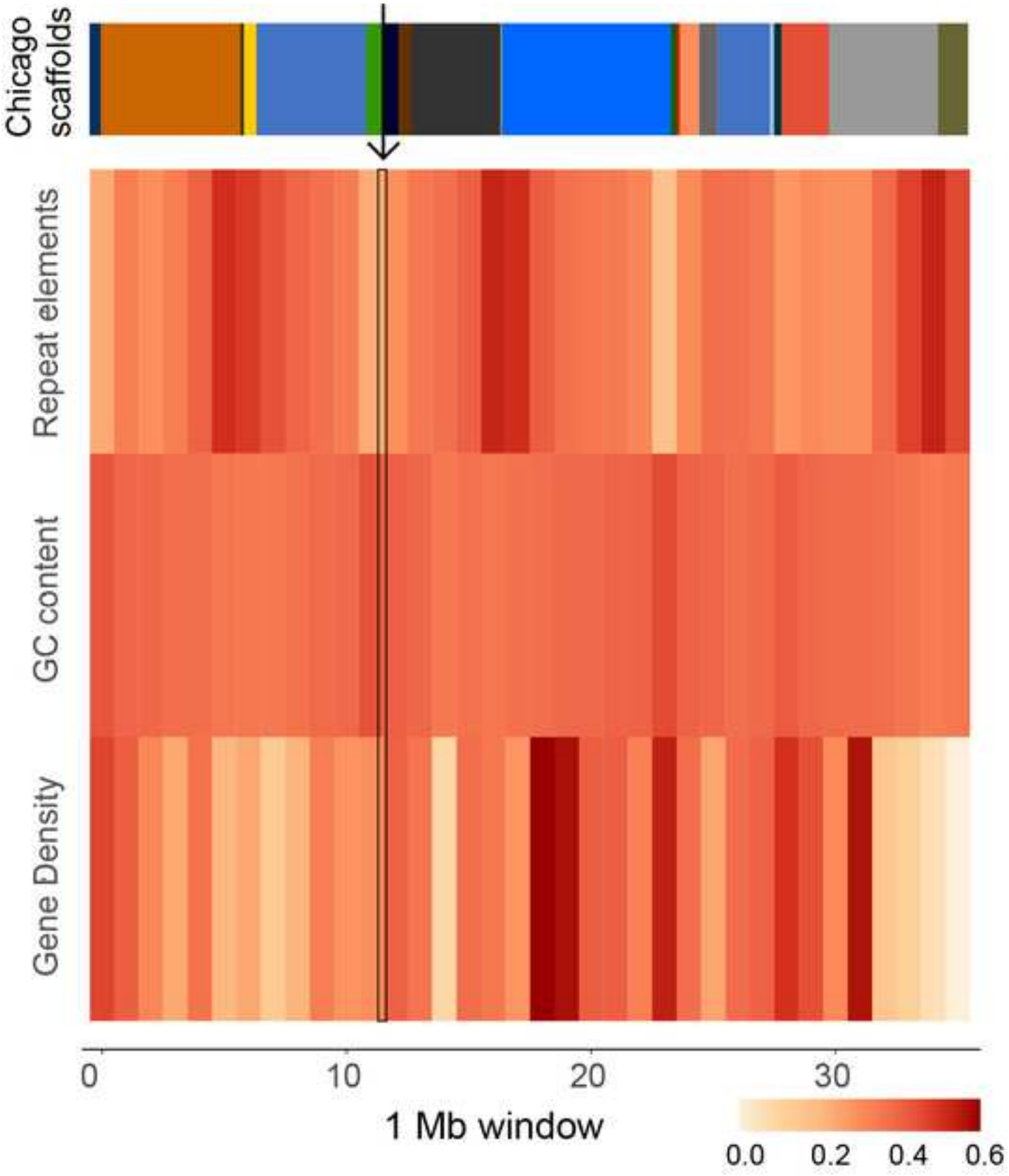

FigurS4

Click here to access/download;Figure;FigureS4.jpg